# Genetic Disruption of Serine Biosynthesis is a Key Driver of Macular Telangiectasia Type 2 Etiology and Progression

Roberto Bonelli,[1,2] Brendan R E Ansell,[1,2] Luca Lotta,[3] Thomas Scerri,[1,2] Traci E Clemons,[4] Irene Leung,[5] The MacTel Consortium,[6] Tunde Peto,[7] Alan C Bird,[8] Ferenc Sallo,[9] Claudia Langenberg,[3] and Melanie Bahlo*[1,2].

1 Department of Medical Biology, The University of Melbourne, 3052, Parkville, Victoria, Australia.
2 Population Health and Immunity Division, Walter and Eliza Hall Institute of Medical Research, 3052, Parkville, Victoria, Australia.
3 MRC Epidemiology Unit, University of Cambridge, CB2 0SL, Cambridge, UK.
4 The EMMES Corporation, Rockville, 20850, Maryland, United States.
5 Department of Research and Development, Moorfields Eye Hospital NHS Foundation Trust, EC1V 2PD, London, United Kingdom.
6 A list of members and affiliations is provided in **Table S8**.
7 Department of Ophthalmology, Queen's University, Belfast, BT7 1NN, United Kingdom.
8 Inherited Eye Disease, Moorfields Eye Hospital NHS Foundation Trust, EC1V 2PD, London, United Kingdom.
9 Department of Ophthalmology, University of Lausanne, Hôpital Ophtalmique Jules-Gonin, Fondation Asile des aveugles, Switzerland.
* Correspondence: bahlo@wehi.edu.au, +61 03 9345 2555

# Abstract

**Purpose**

Macular telangiectasia type 2 (MacTel) is a rare, heritable and largely untreatable retinal disorder, often comorbid with diabetes. Genetic risk loci subtend retinal vascular calibre, and glycine/serine/threonine metabolism genes. Serine deficiency may contribute to MacTel via neurotoxic deoxysphingolipid production, however an independent vascular contribution is also suspected. Here we use statistical genetics to dissect the causal mechanisms underpinning this complex disease.

**Methods**

We integrated genetic markers for MacTel, vascular, and metabolic traits, and applied Mendelian randomization, MTAG, and conditional/interaction genome-wide association analysis to discover causal contributors to both disease, and spatial retinal imaging sub-phenotypes.

**Results**

Serine was a key causal driver of disease occurrence and progression, with a lesser contribution to type 2 diabetes risk. Conversely, glycine, threonine and retinal vascular traits are unlikely to be causal for MacTel. Conditional regression analysis resolved three novel disease loci independent of endogenous serine biosynthetic capacity. By aggregating retinal phenotypes into endophenotypes, we demonstrate that SNPs constituting independent risk loci act via related endophenotypes.

**Discussion**

Our findings will aid in early diagnosis and accurate prognosis of MacTel, and improve prospects for effective therapeutic intervention. Our integrative genetics approach also serves as a useful template for post-GWAS analyses in other disorders.



Retinal Disease | Mendelian Randomization | Metabolomics | GWAS | Serine

# Introduction

## MacTel Disease and previous GWAS study

Macular telangiectasia type II (MacTel [1]), is a rare degenerative eye disease affecting the macula [2,3]. MacTel is bilateral and progressively affects visual acuity [4,5], reading ability [6], and vision-related quality of life [7,8]. A successful phase II clinical trial has recently been reported for an intravitreal encapsulated cell therapy implant, showing efficacy in slowing disease progression [9]. However, less invasive, non-surgical and more economical therapies are lacking. Given the rarity of MacTel and its subtle clinical signs, often requiring several ophthalmological diagnostic methods, the disease has been largely under/misdiagnosed [4]. Hence further insight into the genetic basis of MacTel is key for accurate diagnosis, identifying future therapies, developing predictive models for the disease, and increasing prognostic accuracy.

We previously published the first genome-wide association study on 476 MacTel patients and 1733 controls [10], identifying and replicating five loci. A single nucleotide polymorphism (SNP) at locus 5q14.3 (rs73171800) showed the strongest association with the disease and was previously identified to be associated with the quantitative traits of retinal venular and arterial calibre [11,12]. The other four loci, 1p12 (rs477992), 2q34 (rs715), 7p11.2 (rs4948102), and 3q21.3 (rs9820286) were implicated in glycine and serine metabolism [13,14]. Importantly, loci 3q21.3 and 7p11.2 did not reach genome-wide significance, and the SNPs at locus 3q21.3 were only in proximity, but not in linkage disequilibrium (LD) with those associated with MacTel. In this GWAS we measured and found significant depletion of serum serine, glycine and threonine in MacTel patients compared to controls. These data provided the first insight into the genetic complexity underpinning MacTel, and highlighted the potential involvement of metabolic and vascular trait disturbances in disease aetiology.

Glycine and serine are essential amino acids involved in many fundamental biochemical reactions. Some of the most well-known biochemical pathways relying on glycine and serine are the sphingolipid metabolism pathway (KEGG:map00600) and the glycerophospholipid pathway (KEGG:map00564). Pathogenic variants in genes involved in serine and glycine synthesis lead to severe congenital disorders such as phosphoglycerate dehydrogenase deficiency (*PHGDH*, 601815) and glycine encephalopathy (*GLDC*, 605899). Glycine and serine can be synthesized from one another as well as from other metabolic compounds such as sarcosine and hydroxypyruvate. Additionally, they can both be obtained through dietary intake.

A recent study reported the co-occurrence of MacTel in patients with a rare neuropathy, hereditary sensory and autonomic systemic neuropathy type I,,orHSAN1 (162400) [15]. This neuropathy results from loss of function mutations in the enzyme serine palmityltransferase, leading to accumulation of neurotoxic deoxysphingolipids. A similar accumulation of deoxysphingolipids was demonstrated in MacTel patients, but unlike HSAN1, was attributed to systemic serine deficiency.

MacTel is often comorbid with type 2 diabetes (T2D) [16]. It is unknown whether traits such as metabolite abundances, T2D, or retinal vascular calibre, now known to be associated with MacTel, are causative or merely associated with the disease for other reasons. Causation hypotheses are now routinely investigated using Mendelian Randomization (MR). MR borrows from Instrumental Variable (IV) analysis and assumes that if a disease is caused by a particular intermediate phenotype, and the latter is caused by genetic variants, then the same genetic variants should be also associated with the disease [17–19]. Genetic variants involved in retinal vascular calibre traits and T2D have been previously identified [11,12,20] and the largest metabolomic GWAS meta-analysis to date recently identified almost 500 loci that are associated with differences in 142 serum metabolite levels in humans [21,22]. The results from these studies can be used to investigate causal drivers of MacTel susceptibility via the MR approach.

GWA studies on rare complex traits such as MacTel are inevitably underpowered due to the difficulty in recruiting a large number of samples. However, well-powered GWAS are now collated in resources such as the European Bioinformatics Institute GWAS catalogue. Methods leveraging such resources to aid underpowered GWA studies have now been developed. An example is Multi-Trait Association GWAS (MTAG) [23] which exploits the genetic correlation between traits to identify new loci.

Progress in MacTel diagnosis and treatment is complicated by a lack of clear indicators of early stages of the disease and by the substantial inter-patient and interocular heterogeneity of retinal phenotypes. Apportioning genetic variation to separate retinal malformations has the potential to shed light on the different biological mechanisms via which each locus contributes to the disease. Performing joint genetic and retinal phenotypic data can investigate whether different retinal abnormalities are consequences of common or largely independent biological perturbations.

In this study, we test for the causality of several traits on MacTel disease (**Figure 1A**). We exploit independent studies on MacTel-related traits to increase discovery power in our disease cohort, and both identify new disease loci while further resolving previously identified loci (**Figure 1B**). We use extensive retinal phenotypic data from MacTel patients to identify key genetic drivers of specific subphenotypes (**Figure 1C**). We collate genetic loci into functional groups by testing their combined effects on ocular spatial phenotypes (**Figure 1D**). This study represents the first integrated analysis of MacTel genotypic data with MacTel-related traits as well as retinal imaging phenotypic data. Our study serves as a model for post-GWAS studies with phenotyping datasets.

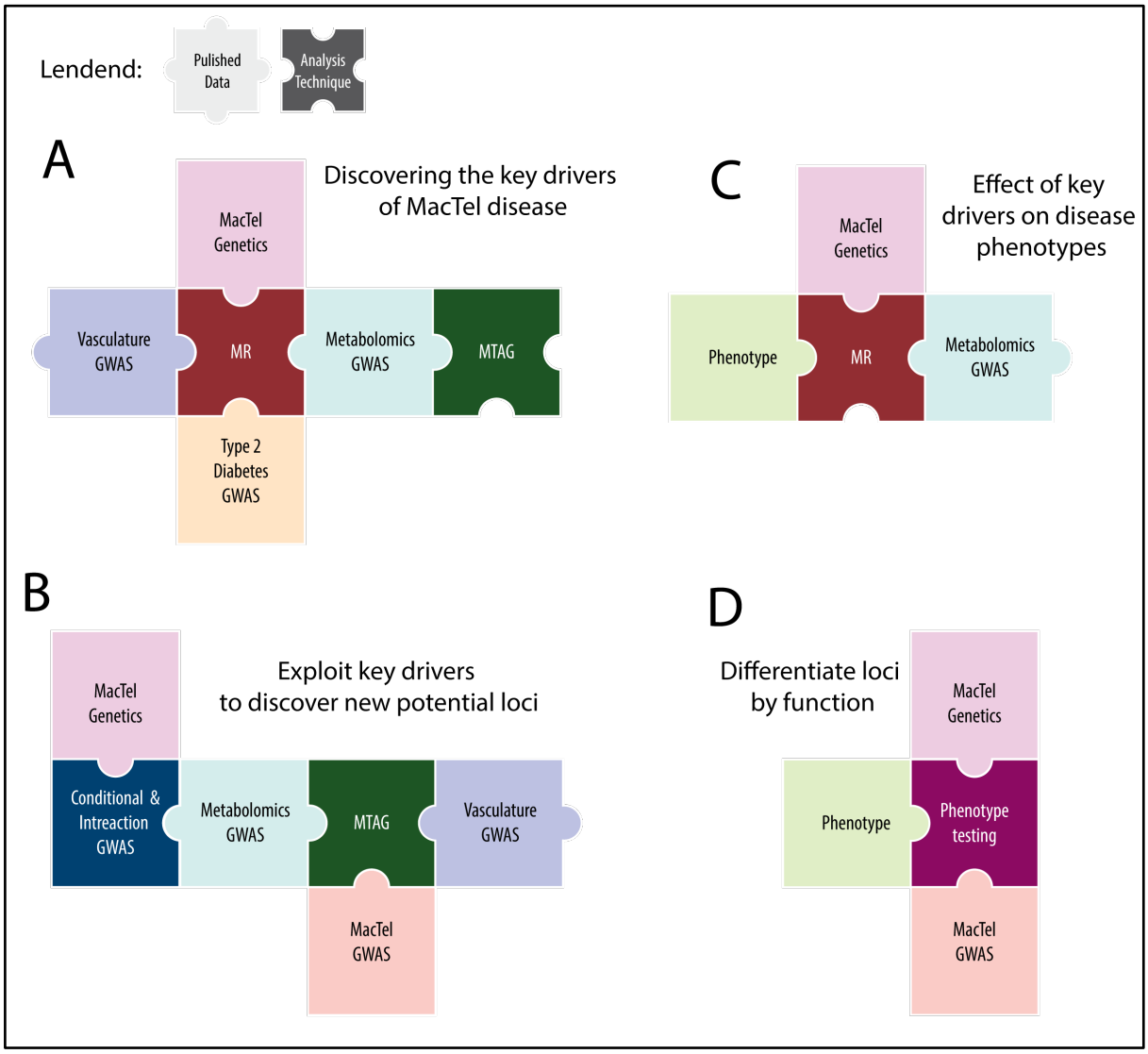


**Figure1:** Study conceptual map. Each panel represents a study aim and depicts the data and the analysis technique used. Data is presented as pastel color pieces with black typing while analysis techniques are presented as darker panels with white writing. MacTel genetics refers to individual level SNP data available from our previous GWAS study. MacTel GWAS refers to the MacTel GWAS summary statistics. Vasculature GWAS refers to the summary statistics data available from two previous retinal vasculature calibre genetic studies [11,12]. Metabolomics GWAS refers to summary statistics data available from a recently published metabolomics GWAS [21,22]. T2D GWAS refers to summary statistics data available from GWAS study on T2D [20]. MTAG: Multi-Trait Association GWAS; MR: Mendelian Randomization.

# Methods

Unless otherwise stated, all statistical and computational analyses were performed using the R statistical software, version 3.5.1. Corrected p-values less than 0.05 were considered statistically significant. For genome-wide association analyses, uncorrected p-values less than 5e-8 were considered genome-wide significant.

## DNA samples and SNP genotyping

Genotypic data was available for 476 MacTel patients and 1733 controls. SNPs were genotyped using the Illumina 5.0M chip as described previously [10]. Retinal phenotypic data was available for 455 patients MacTel patients. Genetic predictors (betas or odds ratios (ORs), with corresponding SNP ID and relevant allele) for metabolites and retinal vascular calibre, were provided by the corresponding authors of each study [11,12,21,22].

## Mendelian Randomization Procedures

To perform Mendelian randomization analysis on MacTel with metabolites, T2D and retinal vasculature we used the allele-score method for individual-level genetic data as described by Burgess et al. 2016 [24]. Using a p-value threshold of 5e-8 we extracted SNPs significantly associated with serum metabolite concentrations or other traits of interest (retinal venular calibre, retinal arteriolar calibre, and T2D). We estimated Genetically Predicted Metabolites (GPMs) and Genetically Predicted Traits (GPTs), for T2D and retinal vasculature (**Table S1**) for each subject by using the magnitudes of the significant SNPs as weights, in the manner of a polygenic risk score (**Supplementary Methods**). We used logistic regression models to test for association between GPMs, or GPTs and MacTel susceptibility. This analysis was corrected for genetically determined sex at birth and the first principal component to account for batch effects including population stratification, as in our previous publication [10]. We used Benjamini-Hochberg multiple testing correction to control the false discovery rate threshold of 5%. A sequential conditional modelling approach was used to identify GPMs independently associated with the disease. Specifically, the most significant GPMs were iteratively added as covariates in the logistic regression model and re-tested until no GPM was nominally significant after FDR correction.

## Conditional and Interaction GWAS and MTAG analysis

Conditional GWAS were performed by including GPMs or GPTs in the logistic regression models as covariates. For the interaction GWAS, an interaction term was included for each SNP and the GPM or GPT combination of interest. Consistent with the original GWAS on this data, each model also included genetically determined sex at birth and the first principal component [10]. Analyses were performed using Plink v1.9 [25]. Results from the conditional and interaction GWAS were analysed using FUMA [26]. LocusZoom plots were produced using the LocusZoom software [27]. MTAG analysis was performed by integrating the available summary statistics for each trait of interest using the MTAG software [23].

## Retinal phenotype clustering

As part of the Natural History Observation and Registry studies of Macular Telangiectasia [28], longitudinal retinal phenotypic data (colour fundus images, optical coherence tomography and fluorescein angiographic images) was collected 2005-2015 from 1,716 patients (3,410 eyes). The data consisted of 143 spatial measurements of retinal phenotypes (**Table S2)**. A detailed

195 description of the corresponding methods can be found elsewhere [28]. Each phenotype was
196 measured in 9 different sub-fields of the retina (defined by the ETDRS grid [29] **Figure S1**). The
197 phenotype data was cleaned by performing missing data imputation (**Supplementary**
198 **Methods**). The cleaned dataset contained 119 phenotypes that were collapsed into 30
199 biologically relevant endophenotypes using factor analysis (**Supplementary Methods**).

## 200 Investigating the relationship of retinal endophenotypes with 201 genetic drivers

202 We tested for association between retinal endophenotypes and significant disease-associated
203 GPMs, GPTs and prioritised SNPs. The dataset containing retinal endophenotypes and
204 genetic information included 3,280 observations from 455 MacTel patients (907 eyes in total)
205 with an average of 3.6 observations per eye over 10 years. Association testing was performed
206 using a linear mixed model approach, assuming an additive effect of SNP alleles that
207 increased MacTel risk. P-values were corrected using an adaptive Benjamini-Hochberg
208 procedure [30]. Further details are provided in **Supplementary Methods**.
209

# 210 Results

211

## 212 Discovering key drivers of MacTel disease: Metabolites

213 The MR procedure (**Figure 1A**) applied to the metabolite panel highlighted 14 GP metabolites
214 significantly associated with MacTel **Table 1**. A list of all metabolite associations is provided
215 in **Table S3**. The two most significant metabolites were GP serine and GP glycine In contrast
216 to the metabolomics results from our previous metabolomics study with directly measured
217 metabolites, GP threonine was not significant. Other significant metabolites included GP
218 arginine, GP phenylalanine and GP phosphatidylcholine species. GP alanine was borderline
219 significant.
220
221 The significant GPMs correlated with each other in our sample (**Figure S2**), mirroring
222 correlations observed with directly measured metabolite abundances. When all GPMs were
223 re-tested in a model including GP serine as a covariate, GP glycine was the only associated
224 metabolite (**Table S3**) suggesting that the effect of GP glycine on MacTel is largely due to
225 biochemical interactions with serine. GP serine remained significant when included alongside
226 GP glycine. No other GP metabolites remained significant once GP serine and GP glycine had
227 been included (**Table S3**).
228
229

230

| GP Metabolite / Trait | Beta | OR | 95% C.I. | P-value | Biochemical Family |
|---|---|---|---|---|---|
| Serine | -0.65 | 0.52 | 0.46 - 0.58 | 8.38E-28 | Amino Acids and Biogenic Amines |
| Glycine | -0.58 | 0.56 | 0.50 - 0.63 | 5.44E-19 | Amino Acids and Biogenic Amines |
| lysoPhosphatidylcholine acyl C14:0 | 0.21 | 1.23 | 1.11 - 1.37 | 2.48E-03 | Glycerophospholipids |
| Phosphatidylcholine diacyl C32:1 | 0.21 | 1.23 | 1.11 - 1.37 | 2.48E-03 | Glycerophospholipids |
| Phosphatidylcholine diacyl C34:1 | 0.21 | 1.23 | 1.11 - 1.37 | 2.48E-03 | Glycerophospholipids |
| Phosphatidylcholine with acyl-alkyl residue C38:1 | 0.20 | 1.22 | 1.10 - 1.36 | 2.97E-03 | Glycerophospholipids |
| Arginine | 0.17 | 1.18 | 1.07 - 1.31 | 2.83E-02 | Amino Acids and Biogenic Amines |
| Phenylalanine | -0.17 | 0.85 | 0.76 - 0.94 | 2.85E-02 | Amino Acids and Biogenic Amines |
| Arteriolar Retinal Calibre | 0.32 | 1.38 | 1.25 - 1.52 | 2.22E-10 | Vasculature Trait |
| Venular Retinal Calibre | 0.18 | 1.19 | 1.08 - 1.32 | 7.00E-04 | Vasculature Trait |
| T2D | 0.17 | 1.19 | 1.07 - 1.33 | 7.72E-04 | Comorbidity |

231
232 **Table 1**: Significant associations between GPMs and GPT and MacTel. Regression coefficients are presented in
233 the "Beta" column. Odds Ratios (OR) are relative to a single standard deviation increase on the GPM/GPT scale.
234 Odds Ratios 95% confidence intervals are shown in the column 95% C.. Benjamini-Hochberg adjusted P-values
235 are presented under the column P-value.
236
237
238 The GWAS used to predict the genetic complement of serine was underpowered compared
239 to the glycine GWAS[22] (**Supplementary Materials**). However, biochemically-based genetic
240 correlation exists between the two. Hence, we attempted to boost the power of the serine
241 GWAS results by combining them with the glycine GWAS results in an MTAG analysis (**Figure**
242 **1A**). The newly identified MTAG serine loci were used to construct a new and more powerful
243 genetic predictor of serine (GP MTAG serine, **Table S1**). We found that GP MTAG serine
244 encompassed the entire metabolic predictive signal for MacTel, as the original GP glycine was
245 no longer required in the model once GP MTAG serine was included. Further MR testing of a
246 broader set of 248 GP metabolite abundances using results from Shin et al [14,31] (**Table S1**)
247 found a few additional significant univariate contribution from other metabolites

(**Supplementary Materials** and **Table S4**). However, none remained significant after inclusion of GP serine as a covariate.

# Discovering key drivers of MacTel disease: T2D and retinal vasculature

Genetically predicted T2D was significantly associated with MacTel, as were both GP arteriolar and venular calibre when tested separately. However, the vasculature trait results were driven by a single SNPs: rs2194025 (for arteriolar calibre) and rs17421627 (for venular calibre), both in strong LD with SNP rs73171800 at 5q14.3 previously identified in our original GWAS [10]. When including both vascular traits in the same model, only arteriolar calibre remained significant, due to the reduced number of SNPs (N = 2) used to construct that GPT (**Figure S3**). When GPTs for retinal arteriolar calibre and T2D were included in a model with GP glycine and serine, all remained significant.

As a quality control analysis, we compared the effect sizes for each instrumental SNP on both MacTel and the metabolites or traits to inspect for potential SNP outlier effects of pleiotropy (**Figure 2**). A negative, linear relationship was detected between the effect on metabolic abundance and MacTel risk for the SNPs used to define glycine and serine. A positive relationship was observed for T2D and vasculature traits, while no relationship was detected for threonine which was used as a control trait, where no significant association was observed. We additionally observed that the regression line for all significant traits except the vasculature related traits, did not have intercept terms that were significantly different from 0 ($b_{0,serine}$= –0.07, p=0.2 ; $b_{0,glycine}$=0.070, p=0.131 ; $b_{0,T2D}$=0.002, p=0.88) suggesting a non-pleiotropic effect of the instruments used to test such traits[32]. The same conclusion was drawn when Glycine and T2D SNPs considered to have potential outlier effects were removed.

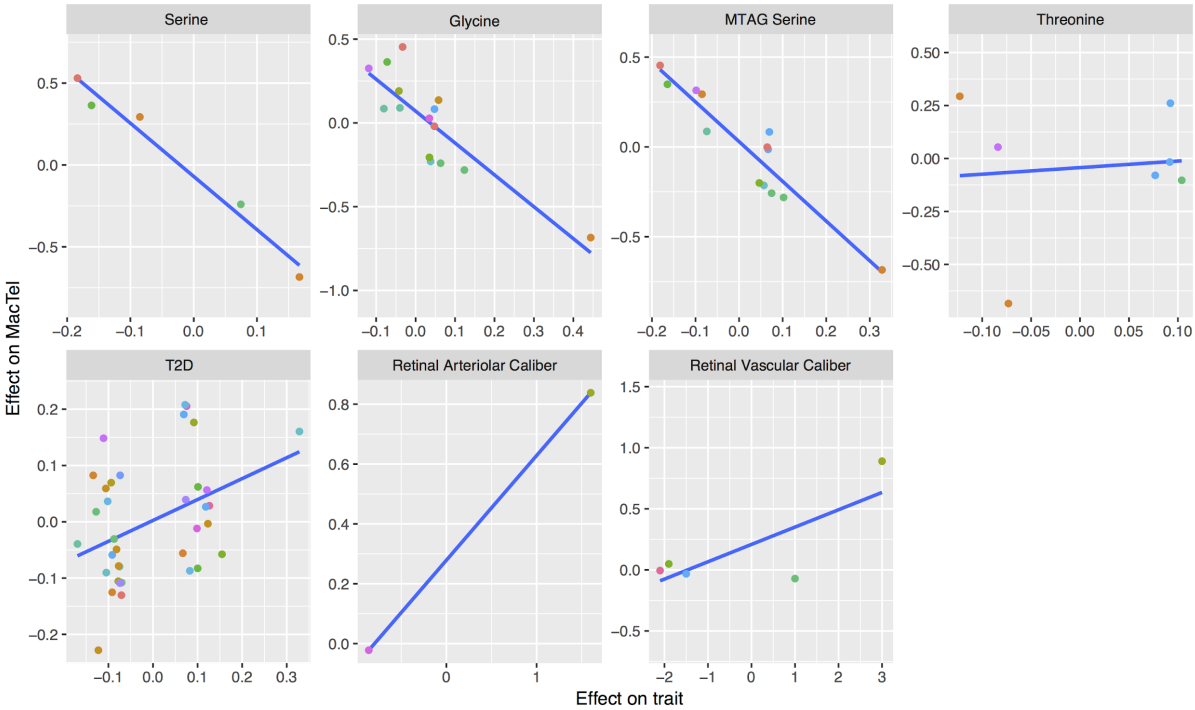


**Figure 2:** Effect size comparisons between MacTel and specific trait of SNPs used to define GPM and GPT. Each dot represents a SNP. Each panel represents a traits and contains the SNPs that were found to have a genome-wide significant effect on that trait. The x-axis captures the effect sizes of the SNPs on the trait while the y-axis captures the effect of the same SNPs on MacTel risk. The blue line represents a simple regression line between the two. Metabolites or traits causally affecting the disease are expected to have correlated effect sizes. Colour of the dots represents chromosomal positions where different chromosomes are represented by different colours.

# Using causal traits to discover new disease susceptibility loci for MacTel

## MTAG results

To discover new loci putatively involved in MacTel, we performed MTAG analysis by including GWAS summary statistics for glycine, serine, retinal venular calibre, and retinal arteriolar calibre along-side MacTel (**Figure 1B**). T2D was not included as genome-wide summary statistics were not available. The number of SNPs shared across all datasets was 799,436 (maximal FDR = 0.397). This analysis confirmed the three previously identified MacTel risk loci [10] and revealed 5 novel loci attaining genome-wide significance (**Table 2, Table S5** for details).

| rsid | Locus | Candidate Gene | MTAG P-val MacTel | New GW. | P-val Art | P-val Ven | P-val Gly | P-val Ser | P-val MacTel |
|---|---|---|---|---|---|---|---|---|---|
| | | | | | Sim et al 2013 | Ikram et al 2010 | Lotta et al 2019 | Lotta et al 2019 | Scerri et al 2017 |
| rs3815630 | 2q34 | *CPS1* | **7.62E-143** | No | *1.51E-01* | *6.23E-01* | **2.23E-308** | **6.50E-31** | **4.43E-08** |
| rs1035387 | 5q14.3 | *TMEM161B-AS1* | **1.16E-16** | No | **1.50E-09** | **1.15E-08** | *5.43E-01* | *7.53E-01* | **1.16E-16** |
| rs477992 | 1p12 | *PHGDH* | **2.21E-15** | No | *7.44E-01* | *7.95E-04* | **6.09E-07** | **2.01E-80** | **2.60E-12** |
| rs4543497 | 7p11.2 | *PSPH* | **2.22E-15** | Yes | *3.56E-01* | *2.07E-01* | **9.01E-28** | **3.29E-54** | 8.11E-06 |
| rs4841132 | 8p23.1 | *LOC157273* | **8.43E-14** | Yes | *5.55E-02* | *2.95E-02* | **1.73E-34** | 1.23E-04 | 4.54E-02 |
| rs1563075 | 16q23 | *GCSH* | **1.79E-13** | Yes | *6.86E-01* | *3.77E-01* | **2.57E-28** | 1.19E-01 | 4.66E-03 |
| rs2954021 | 8q24.1 | *TRIB1* | **1.53E-12** | Yes | *3.89E-01* | *6.33E-01* | **2.35E-21** | **2.40E-10** | 8.70E-05 |
| rs4742212 | 9p24 | *GLDC* | **1.19E-09** | Yes | *4.73E-01* | *6.88E-01* | **3.06E-34** | 1.69E-04 | 2.82E-01 |

**Table 2**: Genome-wide significant loci for MacTel from MTAG analysis using retinal venular (Ven) and arteriolar (Art) calibre, serine (Ser) and glycine (Gly). Novel genome-wide significant loci are identified by the column New GW. Bold text indicates genome-wide significant P-values on respective original studies. Grey italicised p-values are associations expected to be null *a priori*.

Among the five new genome-wide significant loci was locus 7p11.2 which did not reach genome-wide significance in the original GWAS but was deemed important given its established relationship with glycine and serine [10]. We did not observe any significant MTAG results for locus 3q21.3, originally proposed to affect MacTel though a connection with glycine and serine [10]. This SNP was in fact not genome-wide significant for either glycine (p = 0.041) or serine (p = 0.65) and is likely to present either a false positive or a GWAS signal not contributed to by glycine or serine.

## Conditional and Interaction GWAS

To uncover genetic correlates of MacTel independent of glycine and serine, we performed a GWAS conditioning on these genetically predicted traits (**Figure 1B**). This analysis identified four genome-wide significant peaks (**Figure S4 a)**.

As expected, the original signal on locus 5q14.3 (rs73171800) related to vascular calibre, remained significant, confirming the independence of this locus from genetic drivers of serine and glycine. A second genome-wide significant signal on locus 3p24.1 (rs35356316, p = 3.10e-08) was identified and was situated in a ‘gene desert’ proximal to the genes *EOMES*

322 and *SLC4A4*. Another single SNP in very close proximity to rs35356316 reached genome-
323 wide significance as in the original MacTel GWAS study [10] but was believed to be a false
324 positive, given the lack of LD with any other significant SNP (**Figure S4 b**).
325
326 The remaining two conditionally significant SNPs tagged independent signals in locus 19p13.2
327 (**Figure S4 c-d**). SNP rs36259 is an exonic non-synonymous SNP located in the *CERS4* gene
328 which achieved close to genome-wide significance (p=6.270e-08) and was nominally
329 significant in our original study (p = 1.69e-7). In close proximity, we found an independent
330 intergenic SNP rs4804075 (p = 3.72e-07) which lacked evidence of an eQTL effect on any
331 neighbouring genes, and which did not reach genome-wide significance. These results remain
332 significant when conditioning on SNP rs73171800 (locus 5q14.3) and GP T2D.
333
334 We performed additional GWAS analyses testing for interactions between all SNPs with GP
335 serine, glycine, T2D, and SNP rs73171800 (**Figure 1B**). However, no further significant
336 interacting loci were found (**Figure S5 a-d**).
337

## 338 Effect of key drivers on retinal endophenotypes

339 Given the small sample size of the endophenotypic data (N = 455), we decided to only test for
340 association between endophenotypes and GP glycine, serine and T2D, as these bore the
341 clearest association with disease etiology (**Figure 1C, Table S6**). No significant association
342 between GP glycine or T2D and endophenotypes was found after correcting for GP serine,
343 and we, therefore, excluded them from additional testing. High GP serine levels were found to
344 be protective against loss of retinal transparency, leakage at the outer capillary network and
345 the retinal pigment epithelium (RPE) in MacTel progression areas, and leakage at the RPE in
346 the MacTel area. We also found suggestive significance for protection from perivascular
347 pigment clustering in the MacTel area and progression area. Higher GP serine levels were
348 associated with protection from macular thinning in the MacTel area, inferior inner area, and
349 suggestive protection on nasal inner area, and foveal area. Together these results highlight
350 that GP serine is associated not only with MacTel disease risk but also with those retinal
351 endophenotypes characterising disease progression.
352
353

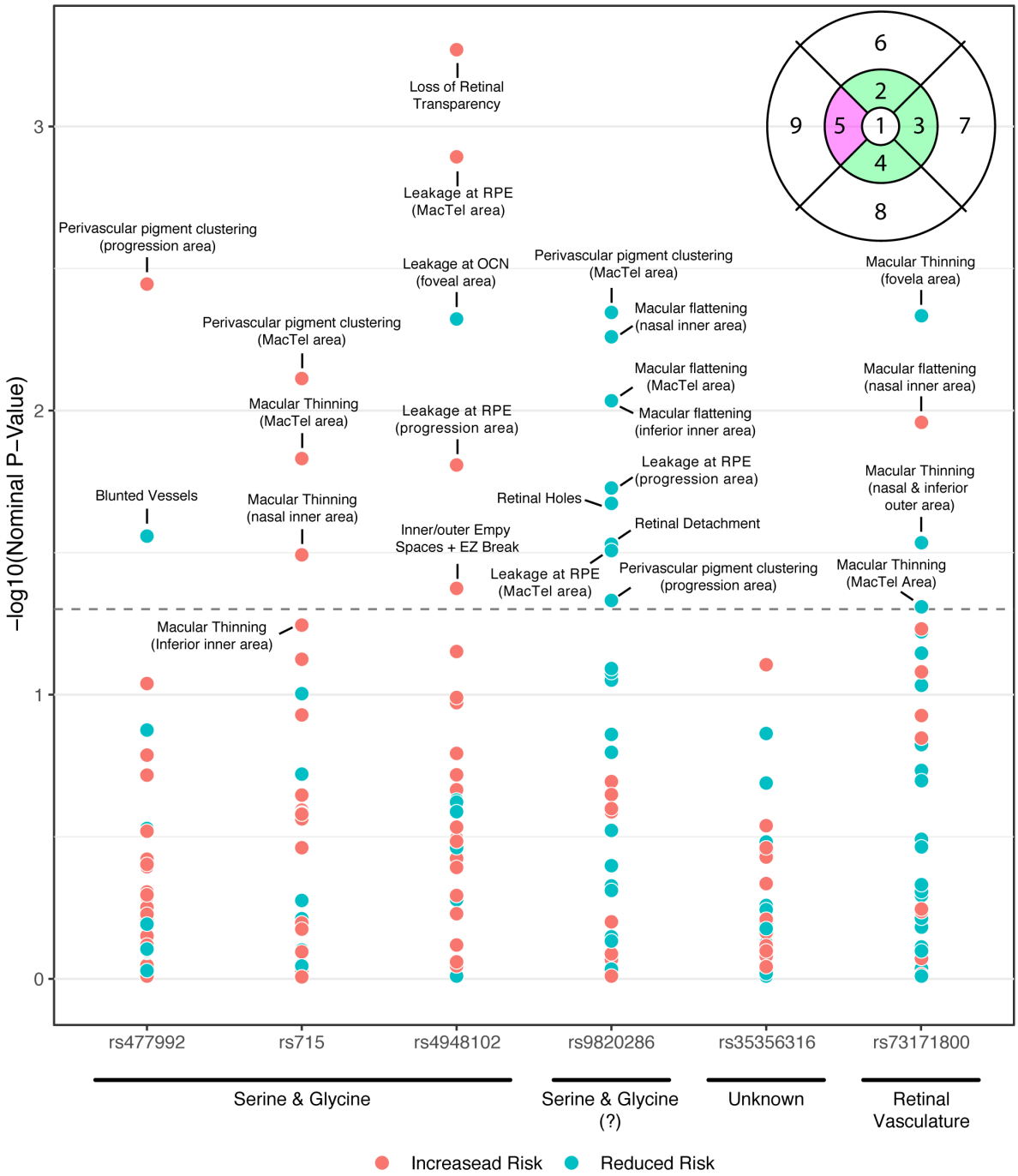


**Figure 3:** Association plot summarising all nominally significant association between MacTel SNPs and the endophenotypes (**Table S6**). SNPs are divided into categories based on MR results. Each dot represents the nominal p-value for each association between all SNPs and endophenotypes. Red dots indicate that MacTel risk alleles for that SNP also increases the risk of the retinal phenotype, while blue dots indicate a reduced risk. The dashed line represents the nominal significance of p=0.05. The top right corner displays the ETDRS grid for the right eye (OD) [29] used to divide the endophenotypes into 9 retinal areas; 1: foveal area, 2: superior inner area, 3: nasal inner area, 4: inferior inner area, 5: temporal inner area, 6: superior outer area, 7: nasal outer area, 8: inferior outer area, and 9: temporal outer area. Although definitions vary across the literature, for simplicity in this manuscript we define the pink area as the 'MacTel [onset] area' while the green areas are MacTel 'progression areas'.

## Determining the effects of GWAS loci on endophenotypes

To determine the likely functional impacts of the original GWAS loci we tested for associations with retinal endophenotypes (**Figure 1D, Figure 3, Table S6**).In No associations remained significant after correction for multiple testing, likely due to the modest sample and effect sizes of individual SNPs on disease endophenotypes. However, using a nominally (uncorrected) significant p-value threshold denoted $p^* < 0.05$ in an exploratory approach, we observed that locus 1p12 (rs477992) was associated with an increased risk of perivascular pigment clustering in the progression area, but protected against risk of blunted vessels. Furthermore, locus 2q34 (rs715) increased the risk of macular thinning in the MacTel area and nasal inner area and the risk of perivascular pigment clustering in the MacTel area. Finally, the MacTel risk allele at locus 7p11.2 (rs4948102) increased the risk of retinal transparency, leakage at the RPE in both the MacTel area and progression area, as well as presence of inner empty spaces and EZ break. This locus however protected against leakage in the outer layer of the foveal area.

These three loci, which converge on glycine/serine metabolism (1p12/rs477992/*PHGDH*, 2q34/rs715/*CPS1*, and 7p11.2/rs4948102/*PSPH*) all demonstrated an overall susceptibility increment to RPE endophenotypes and other macular phenotype risks, lending further support for their role, despite not attaining significance after p-value adjustment.

Interestingly the MacTel risk allele at locus 3q21.3 (rs9820286) was only associated with protection from retinal disease endophenotypes. Specifically, locus 3q21.3 was associated with protection against retinal holes, retinal detachment, perivascular pigment clustering in the MacTel area and progression areas; leakage at the RPE level in the MacTel area and progression area; and foveal slope flattening in MacTel area, inferior inner area, and nasal inner area.

Locus 5q14.3 (rs73171800) corresponded to protection against macular thinning in the foveal area and nasal-inferior outer areas and increased risk of foveal flattening in the nasal inner area. The effect of SNP rs73171800 on macular thickness was consistent with recent findings [33]. We attempted to cluster the loci using hierarchical clustering of their regression coefficients (**Figure S7**). This analysis highlighted the unique endophenotype effect profiles of the 5q14.3 (rs73171800) and 3q21.3 (rs9820286) loci, and their distinctiveness in comparison to the other three loci, known to act on the serine/glycine pathway.

# Discussion

This study exploited well-powered publicly available GWAS data from traits of interest as well as deep retinal phenotyping data to further investigate the genetic aetiology of MacTel, a moderately rare retinal disorder for which the first GWAS was only recently performed [10]. We report causal genetic drivers for MacTel, delineating independent genetically-determined

metabolic contributors to the disease, and quantifying the contribution of MacTel-related traits and genetic risk loci to retinal degeneration.

Mendelian randomization and publicly available data were used to “genetically predict” abundances of different metabolites. Even though all GPMs in this study were generated using estimated SNP allele dosage effects from blood-based metabolomic studies rather than retina, we believe that our results represent a useful approach for interrogating other retinal disorders.

We found genetically-predicted serine depletion as the strongest causal driver of MacTel risk, with an association magnitude much greater than those observed when using single SNPs. This pronounced effect reflects the power of combining multiple genetic variants associated with the disease through a shared biological mechanism; and further emphasizes the causative role of serine in this disease. The direction of association between GP serine and MacTel agrees with results from direct serum serine measurements reported previously [10]. This provides compelling additional evidence for a causal association between serine deficiency and MacTel. Indeed, the MacTel disease odds doubled for every standard unit decrease in GP serine, and individuals in the lowest quintile of GP serine presented an OR of 6.34 for MacTel compared to individuals in the top quintile. Our study results also confirm the pronounced role that serine plays in disease progression. As this analysis was applied only to MacTel patients, the heterogeneity of retinal phenotypes at early disease stages may be under-represented. GP serine was nevertheless able to partly discriminate between subjects with more advanced retinal abnormalities and those without. For example, lower GP serine had a clear association with retinal greying in all retinal areas, which is not observed in all MacTel patients [4]. GP serine also affected retinal thinning in the temporal parafoveal area, a marker of photoreceptor degeneration. Although our results suggest a highly plausible biochemical explanation for differences in disease heterogeneity and progression, we acknowledge that our study used only aggregated retinal phenotypes and proxy measures of progression. Longitudinal data documenting progression is now required to confirm these findings. High concentrations of deoxy-sphingolipids, a byproduct of serine deficiency, have recently been shown to cause MacTel [15]. Our results provide evidence that genetically-encoded serine depletion is causal for MacTel, which likely contributes to the disease by promoting deoxy-sphingolipid biosynthesis [15].

Our results indicate that the association between glycine and MacTel is likely an artefact of the shared genetic signal between this metabolite and serine. This may relate to the considerably greater sample size used to construct the glycine GP, and/or its metabolic dependence on serine. Similarly, the previously observed significant association of threonine to MacTel disease risk [10] is likely due to its metabolic dependence on glycine and serine and thus a bystander effect.

Multi-Trait Association GWAS (MTAG) confirmed the central role of locus 7p11.2 (rs4543497), which was previously found to be only nominally significant, and identified a new locus, 8q24.1 (rs2954021). The latter locus is of great interest since rs2954021 is predictive of endogenous serum serine concentrations [22] and thus might confer MacTel risk by contributing to the same serine pathway as previously identified SNPs. Conversely, we did not find any additional signal arising from shared genetic correlations with retinal vascular calibre traits.

460 Although not significant after correction for multiple testing, we observed a pronounced effect
461 of SNP rs73171800 on macular thickness, specifically, a protective effect of the C allele
462 against macular thinning, which is tantamount to an increase in macular thickness.
463 Interestingly, a large GWAS study previously found that the G allele of SNP rs17421627 -
464 corresponding to the C allele of SNP rs73171800 (LD with rs73171800 $r^2$=0.67), was
465 significantly associated with increased macular thickness [33]. Further, a targeted study of SNP
466 rs17421627, leveraged the deep conservation of this locus to demonstrate enhancer activity
467 which modifies the retinal vasculature. Madelaine et al substituted the homologous zebrafish
468 locus with a construct containing rs17421627, and showed enhancer activity and changed
469 expression of a proximal microRNA, mir-9-2 (homologous with human mir-9-5) [34]. Both mir-9-
470 2 knock-down and endogenous enhancer knock-out animals showed dysmorphic retinal
471 vasculature, indicating that rs17421627 may act on miRNA expression to modify the formation
472 of the retinal vasculature in humans[33] Although our MR analysis did not find a causal
473 relationship between retinal vasculature calibre and MacTel, it may be that other features of
474 the vasculature, for example, leakage, branching or integrity, are modified in rs17421627
475 carriers, and account for the gross differences in macular thickness. Further deep phenotyping
476 of the retinal vasculature in these individuals may yield the physiological basis for this
477 phenotype and its impact on MacTel.
478
479 By conditioning on GP serine, glycine and T2D we revealed independent genetic contributors
480 to MacTel. The locus 3p24.1, tagged by SNP rs35356316, lies between *EOMES* (604615) and
481 *SLC4A4* genes (603345). Interestingly, *EOMES* encodes a transcriptional activator which is
482 shown in mouse studies to interact with the retinal transcription factor *Pou4f2* [35]. The
483 downstream gene *SLC4A4* encodes a sodium-coupled bicarbonate transporter which is
484 expressed in Müller glia and the RPE, and functions to balance pH in the subretinal space [36].
485
486 Conditional analysis further revealed SNP rs36259 at locus 19p13.2 which tags an exonic,
487 non-synonymous SNP located within the gene *CERS4* (615334), encoding a dihydroceramide
488 synthase involved in sphingolipid biosynthesis [37]. Just as serine depletion is associated with
489 defective sphingolipid synthesis, this locus may reduce sphingolipid production and thus
490 contribute to MacTel.
491
492 Type 2 diabetics are over-represented among MacTel patients [16]. We found a weak positive
493 association between GP T2D and MacTel risk. A possible explanation for this is that T2D
494 involves major perturbations of patient metabolism. Specifically, a recent meta-analysis of
495 metabolite abundances associated with pre-diabetes and/or T2D, found that glycine depletion
496 tends to occur in this disease [38]. We show that glycine depletion is not likely to be causative
497 for MacTel and is likely to be a consequence of metabolomic co-regularisation
498 counterbalancing the genetically induced serine depletion. We speculate that diabetes may
499 be a consequence rather than a cause of the metabolic phenotype underlying MacTel. Future
500 MR studies may further dissect this interaction but will require a more highly powered MacTel
501 GWAS. Indeed, T2D risk remained significant even after controlling for GP serine and GP
502 glycine, which indicates the possibility of a separate mechanism unrelated to glycine/serine
503 metabolism.
504
505 Our analysis revealed that locus 3q21.3, which was previously believed to act on the disease
506 by modifying serum glycine and serine, is instead likely disconnected from these metabolites,

as is the case for loci 3p24.1 and 5q14.3. Furthermore, these three loci do not cluster with each other, implying that additional potential disease mechanisms exist.

To conclude, by integrating different sources of genetic and phenotypic data related to macular telangiectasia type II with advanced statistical methods, we find evidence that genetically-encoded serine depletion causes disease onset and likely also progression. Further targeted studies of disease progression and experimental validation of serine-independent contributions will resolve the complex aetiology of MacTel and to enhance treatment efficacy. The methods applied here should also serve as a model for dissecting GWAS results, especially for rarer traits.

# Acknowledgments:

We would like to acknowledge the funding support from the Lowy Medical Research Institute. This work was also made possible through the Victorian State Government Operational Infrastructure Support and Australian Government National Health and Medical Research Council (NHMRC) independent research Institute Infrastructure Support Scheme (IRIISS). RB was supported by the Melbourne International Research Scholarship. BREA was supported by an NHMRC early career Fellowship (1157776). MB was supported by an NHMRC Senior Research Fellowship (1102971) and Program Grant (1054618). We are grateful to Dr Saskia Freytag, Dr Anna Quaglieri, Prof Terry Speed, Prof Gordon Smyth, Dr Mari Gantner, Dr Kevin Eade, Dr Martina Wallace, A/Prof Christian Metallo, Prof Martin Friedlander, Dr Tjebo Heeren, Dr Mali Okada, Dr Sasha Woods, Prof Marcus Fruttiger, and Dr Catherine Egan for their extremely helpful contributions that greatly improved the quality of this manuscript. We are especially grateful to Dr Xueling Sim and Prof Wong Tien Yin for kindly sharing their summary data on retinal vascular calibre traits.

# Declaration of Interests

The authors declare no conflict of interest.

# Web Resources

FUMA: http://fuma.ctglab.nl/
Locus zoom: http://locuszoom.org/
Metabolomics GWAS server: http://metabolomics.helmholtz-muenchen.de/gwas/

# References

1. Gass J. Some problems in the diagnosis of macular diseases. In: *Symposium on Retinal Diseases*. ; 1977:268-270.

545 2. Klein R, Blodi BA, Meuer SM, Myers CE, Chew EY, Klein BEK. The prevalence of
546 macular telangiectasia type 2 in the Beaver Dam eye study. *Am J Ophthalmol*.
547 2010;150(1):55-62.e2. doi:10.1016/j.ajo.2010.02.013

548 3. Aung KZ, Wickremasinghe SS, Makeyeva G, Robman L, Guymer RH. The prevalence
549 estimates of macular telangiectasia type 2: the Melbourne Collaborative Cohort Study.
550 *Retina*. 2010;30(3):473-478. doi:10.1097/IAE.0b013e3181bd2c71

551 4. Charbel Issa P, Gillies MC, Chew EY, et al. Macular telangiectasia type 2. *Prog Retin*
552 *Eye Res*. 2013/5;34:49-77. doi:10.1016/j.preteyeres.2012.11.002

553 5. Gass JD, Blodi BA. Idiopathic juxtafoveolar retinal telangiectasis. Update of
554 classification and follow-up study. *Ophthalmology*. 1993;100(10):1536-1546.
555 https://www.ncbi.nlm.nih.gov/pubmed/8414413.

556 6. Finger RP, Charbel Issa P, Fimmers R, Holz FG, Rubin GS, Scholl HPN. Reading
557 performance is reduced by parafoveal scotomas in patients with macular telangiectasia
558 type 2. *Invest Ophthalmol Vis Sci*. 2009;50(3):1366-1370. doi:10.1167/iovs.08-2032

559 7. Lamoureux EL, Maxwell RM, Marella M, Dirani M, Fenwick E, Guymer RH. The
560 longitudinal impact of macular telangiectasia (MacTel) type 2 on vision-related quality of
561 life. *Invest Ophthalmol Vis Sci*. 2011;52(5):2520-2524. doi:10.1167/iovs.10-6568

562 8. Clemons TE, Gillies MC, Chew EY, et al. The National Eye Institute Visual Function
563 Questionnaire in the Macular Telangiectasia (MacTel) Project. *Invest Ophthalmol Vis*
564 *Sci*. 2008;49(10):4340-4346. doi:10.1167/iovs.08-1749

565 9. Chew EY, Clemons TE, Jaffe GJ, et al. Effect of Ciliary Neurotrophic Factor on Retinal
566 Neurodegeneration in Patients with Macular Telangiectasia Type 2: A Randomized
567 Clinical Trial. *Ophthalmology*. October 2018. doi:10.1016/j.ophtha.2018.09.041

568 10. Scerri TS, Quaglieri A, Cai C, et al. Genome-wide analyses identify common variants
569 associated with macular telangiectasia type 2. *Nat Genet*. February 2017.
570 doi:10.1038/ng.3799

571 11. Ikram MK, Sim X, Xueling S, et al. Four novel Loci (19q13, 6q24, 12q24, and 5q14)
572 influence the microcirculation in vivo. *PLoS Genet*. 2010;6(10):e1001184.
573 doi:10.1371/journal.pgen.1001184

574 12. Sim X, Jensen RA, Ikram MK, et al. Genetic loci for retinal arteriolar microcirculation.
575 *PLoS One*. 2013;8(6):e65804. doi:10.1371/journal.pone.0065804

576 13. Xie W, Wood AR, Lyssenko V, et al. Genetic variants associated with glycine
577 metabolism and their role in insulin sensitivity and type 2 diabetes. *Diabetes*.
578 2013;62(6):2141-2150. doi:10.2337/db12-0876

579 14. Shin S-Y, Fauman EB, Petersen A-K, et al. An atlas of genetic influences on human
580 blood metabolites. *Nat Genet*. 2014;46(6):543-550. doi:10.1038/ng.2982

581 15. Gantner ML, Eade K, Wallace M, et al. Serine and Lipid Metabolism in Macular Disease
582 and Peripheral Neuropathy. *N Engl J Med*. September 2019.
583 doi:10.1056/NEJMoa1815111

584 16. Clemons TE, Gillies MC, Chew EY, et al. Medical characteristics of patients with
585 macular telangiectasia type 2 (MacTel Type 2) MacTel project report no. 3. *Ophthalmic*

586 *Epidemiol*. 2013;20(2):109-113. doi:10.3109/09286586.2013.766757

587 17. Davey Smith G, Hemani G. Mendelian randomization: genetic anchors for causal
588 inference in epidemiological studies. *Hum Mol Genet*. 2014;23(R1):R89-R98.
589 doi:10.1093/hmg/ddu328

590 18. Ebrahim S, Davey Smith G. Mendelian randomization: can genetic epidemiology help
591 redress the failures of observational epidemiology? *Hum Genet*. 2008;123(1):15-33.
592 doi:10.1007/s00439-007-0448-6

593 19. Evans DM, Davey Smith G. Mendelian Randomization: New Applications in the Coming
594 Age of Hypothesis-Free Causality. *Annu Rev Genomics Hum Genet*. 2015;16:327-350.
595 doi:10.1146/annurev-genom-090314-050016

596 20. Morris AP, Voight BF, Teslovich TM, et al. Large-scale association analysis provides
597 insights into the genetic architecture and pathophysiology of type 2 diabetes. *Nat*
598 *Genet*. 2012;44(9):981-990. doi:10.1038/ng.2383

599 21. Wittemans LBL, Lotta LA, Oliver-Williams C, et al. Assessing the causal association of
600 glycine with risk of cardio-metabolic diseases. *Nat Commun*. 2019;10(1):1060.
601 doi:10.1038/s41467-019-08936-1

602 22. Lotta LA, Pietzner M, Stewart ID, et al. Cross-platform genetic discovery of small
603 molecule products of metabolism and application to clinical outcomes. *bioRxiv*.
604 February 2020:2020.02.03.932541. doi:10.1101/2020.02.03.932541

605 23. Turley P, Walters RK, Maghzian O, et al. Multi-trait analysis of genome-wide
606 association summary statistics using MTAG. *Nat Genet*. 2018;50(2):229-237.
607 doi:10.1038/s41588-017-0009-4

608 24. Burgess S, Dudbridge F, Thompson SG. Combining information on multiple
609 instrumental variables in Mendelian randomization: comparison of allele score and
610 summarized data methods. *Stat Med*. 2016;35(11):1880-1906. doi:10.1002/sim.6835

611 25. Purcell S, Neale B, Todd-Brown K, et al. PLINK: a tool set for whole-genome
612 association and population-based linkage analyses. *Am J Hum Genet*. 2007;81(3):559-
613 575. doi:10.1086/519795

614 26. Watanabe K, Taskesen E, van Bochoven A, Posthuma D. Functional mapping and
615 annotation of genetic associations with FUMA. *Nat Commun*. 2017;8(1):1826.
616 doi:10.1038/s41467-017-01261-5

617 27. Pruim RJ, Welch RP, Sanna S, et al. LocusZoom: regional visualization of genome-
618 wide association scan results. *Bioinformatics*. 2010;26(18):2336-2337.
619 doi:10.1093/bioinformatics/btq419

620 28. Clemons TE, Gillies MC, Chew EY, et al. Baseline characteristics of participants in the
621 natural history study of macular telangiectasia (MacTel) MacTel Project Report No. 2.
622 *Ophthalmic Epidemiol*. 2010;17(1):66-73. doi:10.3109/09286580903450361

623 29. Mathew R, Sivaprasad S, Florea D, et al. Agreement between time-domain and
624 spectral-domain optical coherence tomography in the assessment of macular thickness
625 in patients with idiopathic macular telangiectasia type 2. *Ophthalmologica*.
626 2013;230(3):144-150. doi:10.1159/000353455

627 30. Benjamini Y, Krieger AM, Yekutieli D. Adaptive linear step-up procedures that control
628 the false discovery rate. *Biometrika*. 2006;93(3):491-507. doi:10.1093/biomet/93.3.491

629 31. metabolomics gwas server. http://metabolomics.helmholtz-muenchen.de/gwas/.
630 Accessed December 4, 2018.

631 32. Bowden J, Davey Smith G, Burgess S. Mendelian randomization with invalid
632 instruments: effect estimation and bias detection through Egger regression. *Int J*
633 *Epidemiol*. 2015;44(2):512-525. doi:10.1093/ije/dyv080

634 33. Gao XR, Huang H, Kim H. Genome-wide association analyses identify 139 loci
635 associated with macular thickness in the UK Biobank cohort. *Hum Mol Genet*.
636 December 2018. doi:10.1093/hmg/ddy422

637 34. Madelaine R, Notwell JH, Skariah G, et al. A screen for deeply conserved non-coding
638 GWAS SNPs uncovers a MIR-9-2 functional mutation associated to retinal vasculature
639 defects in human. *Nucleic Acids Res*. March 2018. doi:10.1093/nar/gky166

640 35. Mao C-A, Kiyama T, Pan P, Furuta Y, Hadjantonakis A-K, Klein WH. Eomesodermin, a
641 target gene of Pou4f2, is required for retinal ganglion cell and optic nerve development
642 in the mouse. *Development*. 2008;135(2):271-280. doi:10.1242/dev.009688

643 36. Pushkin A, Abuladze N, Lee I, Newman D, Hwang J, Kurtz I. Mapping of the human
644 NBC3 (SLC4A7) gene to chromosome 3p22. *Genomics*. 1999;57(2):321-322.
645 doi:10.1006/geno.1999.5781

646 37. Riebeling C, Allegood JC, Wang E, Merrill AH Jr, Futerman AH. Two mammalian
647 longevity assurance gene (LAG1) family members, trh1 and trh4, regulate
648 dihydroceramide synthesis using different fatty acyl-CoA donors. *J Biol Chem*.
649 2003;278(44):43452-43459. doi:10.1074/jbc.M307104200

650 38. Guasch-Ferré M, Hruby A, Toledo E, et al. Metabolomics in Prediabetes and Diabetes:
651 A Systematic Review and Meta-analysis. *Diabetes Care*. 2016;39(5):833-846.
652 doi:10.2337/dc15-2251

653
654
655

# Supplementary Material: Genetic Disruption of Serine Biosynthesis is a Key Driver of Macular Telangiectasia Type 2 Etiology and Progression

## Supplementary Images:

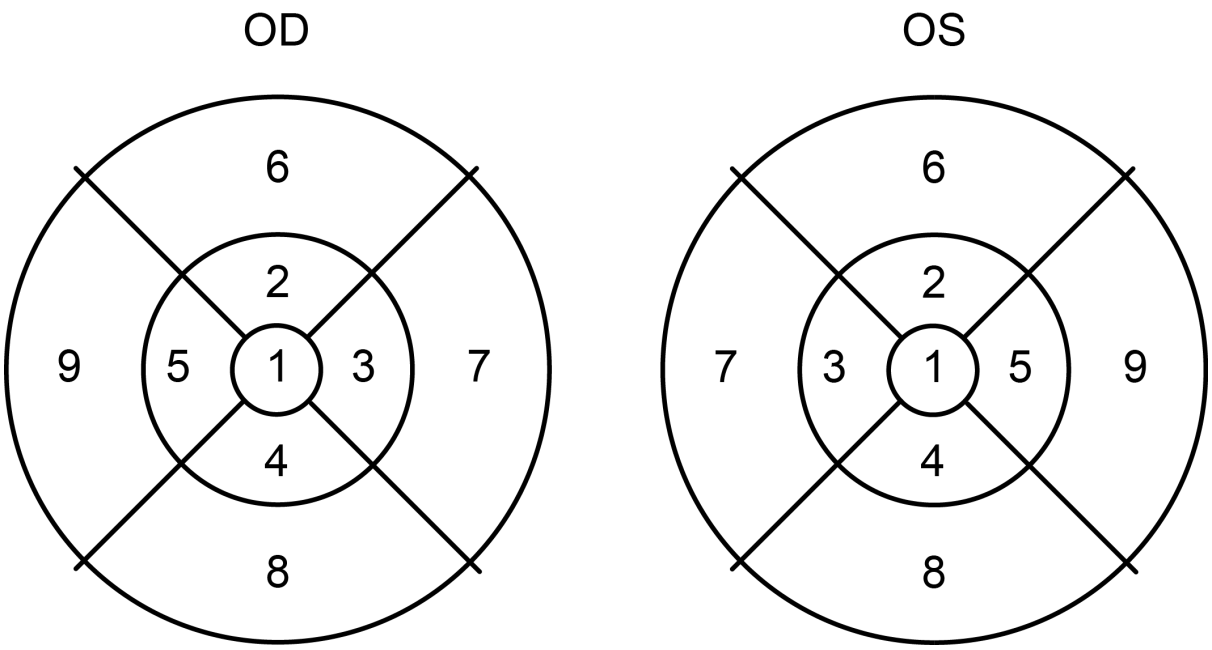


**Figure S1:** Right (OD) and left (OS) eyes macula, were divided into 9 areas according to the ETDRS grid [1]. 1: foveal area, 2: superior inner area (progression area), 3: nasal inner area (progression area), 4: inferior inner area (progression area), 5: temporal inner area (MacTel area), 6: superior outer area, 7: nasal outer area, 8: inferior outer area, and 9: temporal outer area.

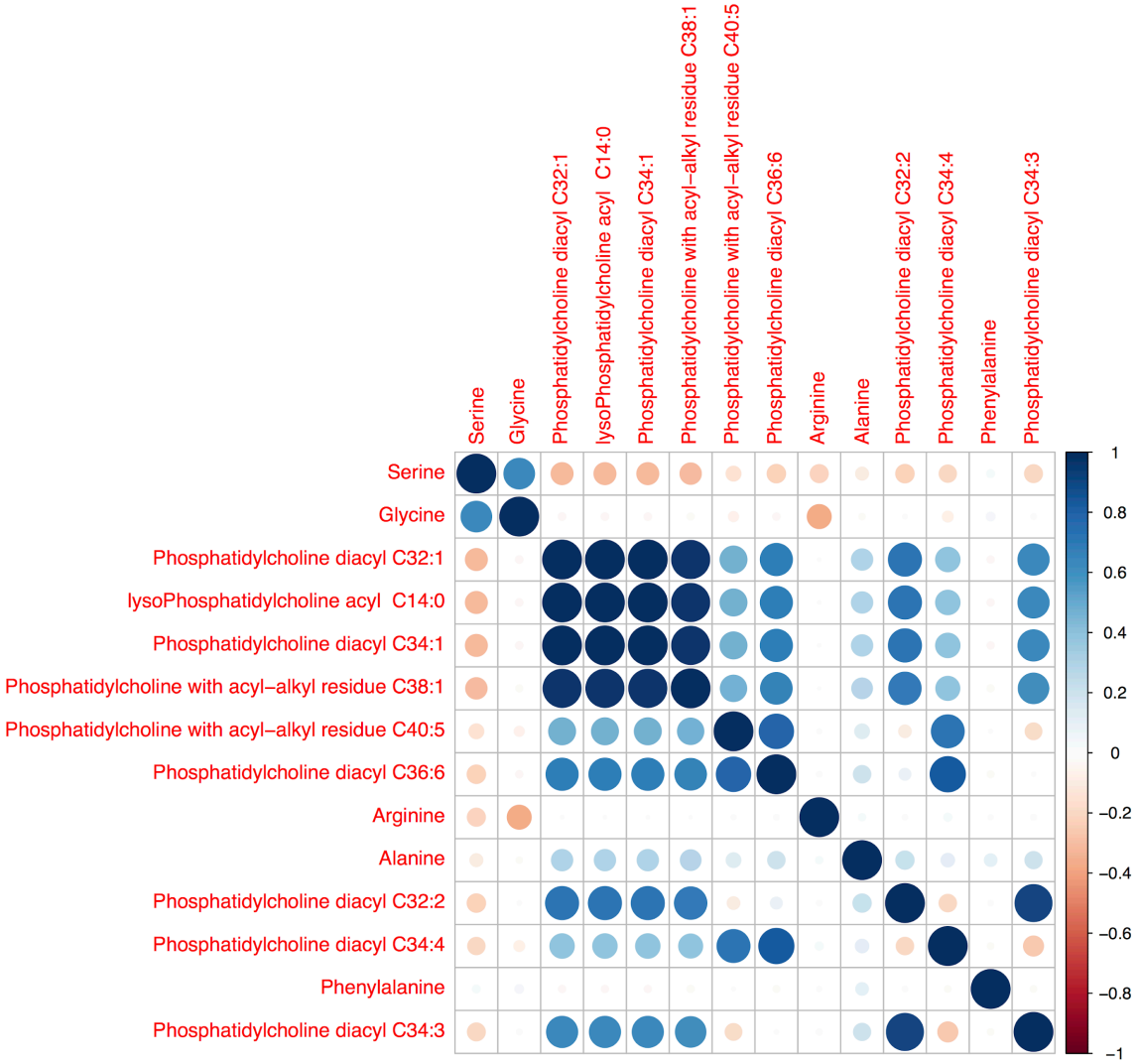


**Figure S2:** Correlation between GPM scores for all GPM scores that achieved multiple testing corrected significance ($p < 0.05$). Bigger dots and saturated colour indicate stronger correlations. Blue indicates a positive correlation while red indicates a negative one.

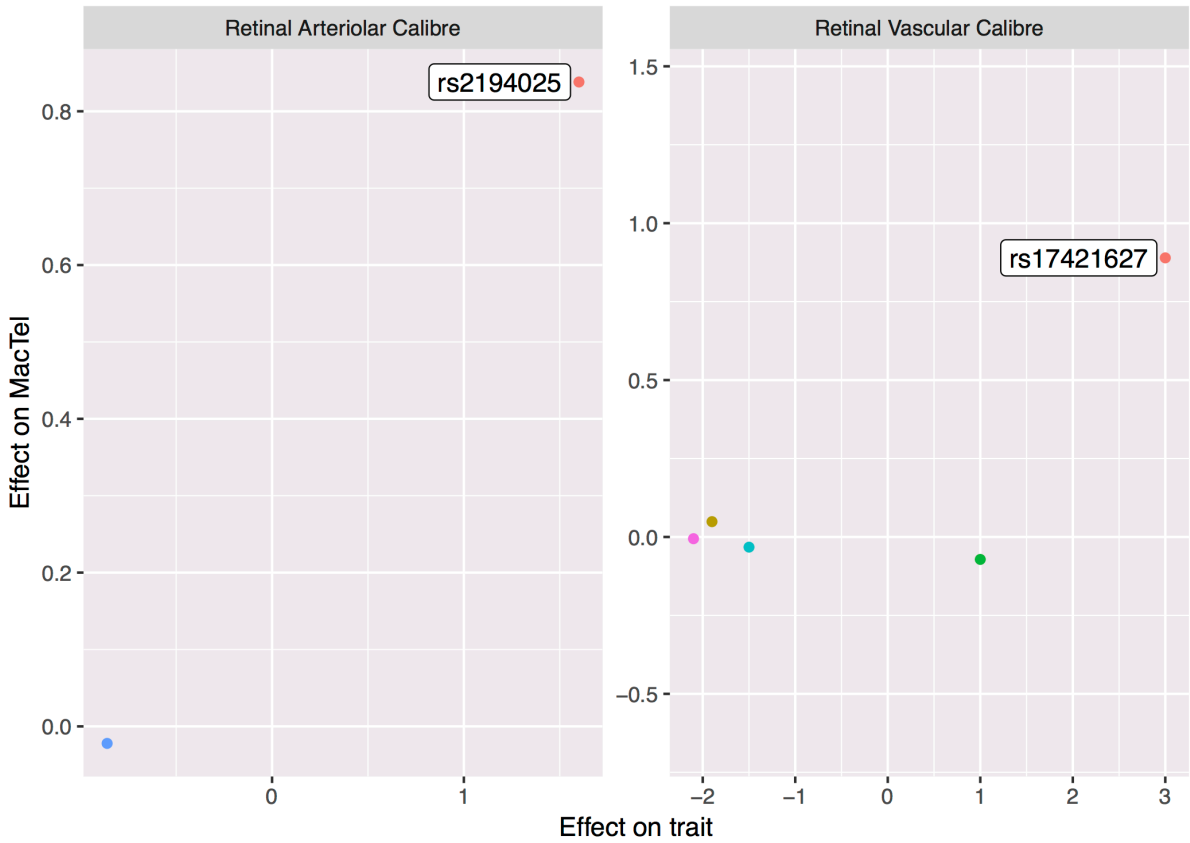


**Figure S3:** Comparison between SNPs effect on vasculature traits and MacTel. Each dot is a SNP which was found to be significantly associated with a vasculature trait. The x-axis represents the effect that the SNP has on the particular trait while the y-axis displays the effect that the SNP has on MacTel. Most SNPs have no effect on MacTel. The only two SNPs that have an effect are the SNPs rs2194025 and rs17421627 which are very close to each other and in strong LD with SNP rs73171800 ($r^2$=0.94 and $r^2$=0.67).

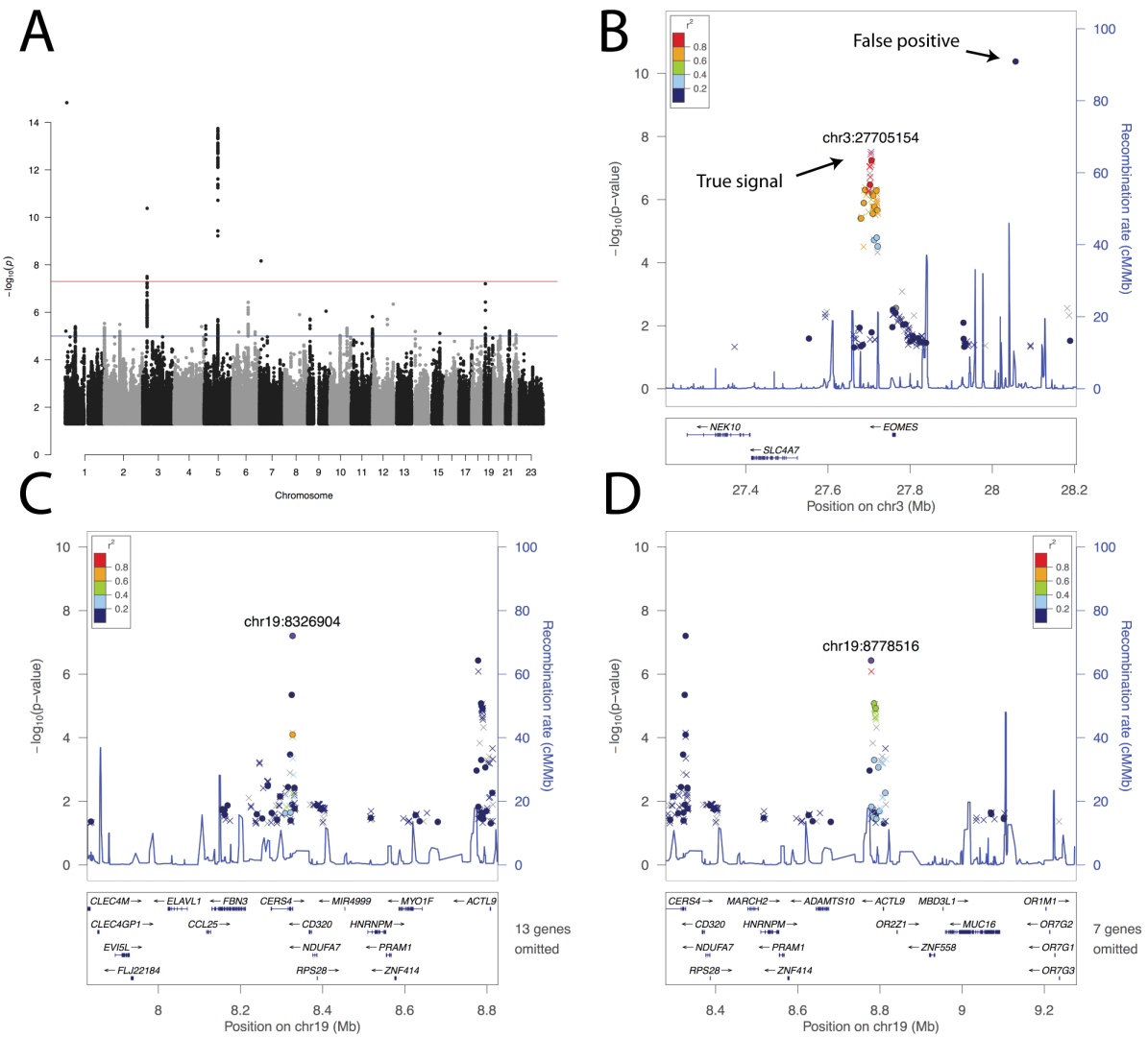


**Figure S4:** MacTel GWAS results conditioned by GP serine and GP glycine. A) Manhattan plot. B) Locus zoom plot of the significant signal on locus 3p24.1. C) Locus zoom plot of the significant signal by SNP rs36259 on locus 19p13.2. D) Locus zoom plot of the significant signal by SNP rs4804075 on locus 19p13.2.

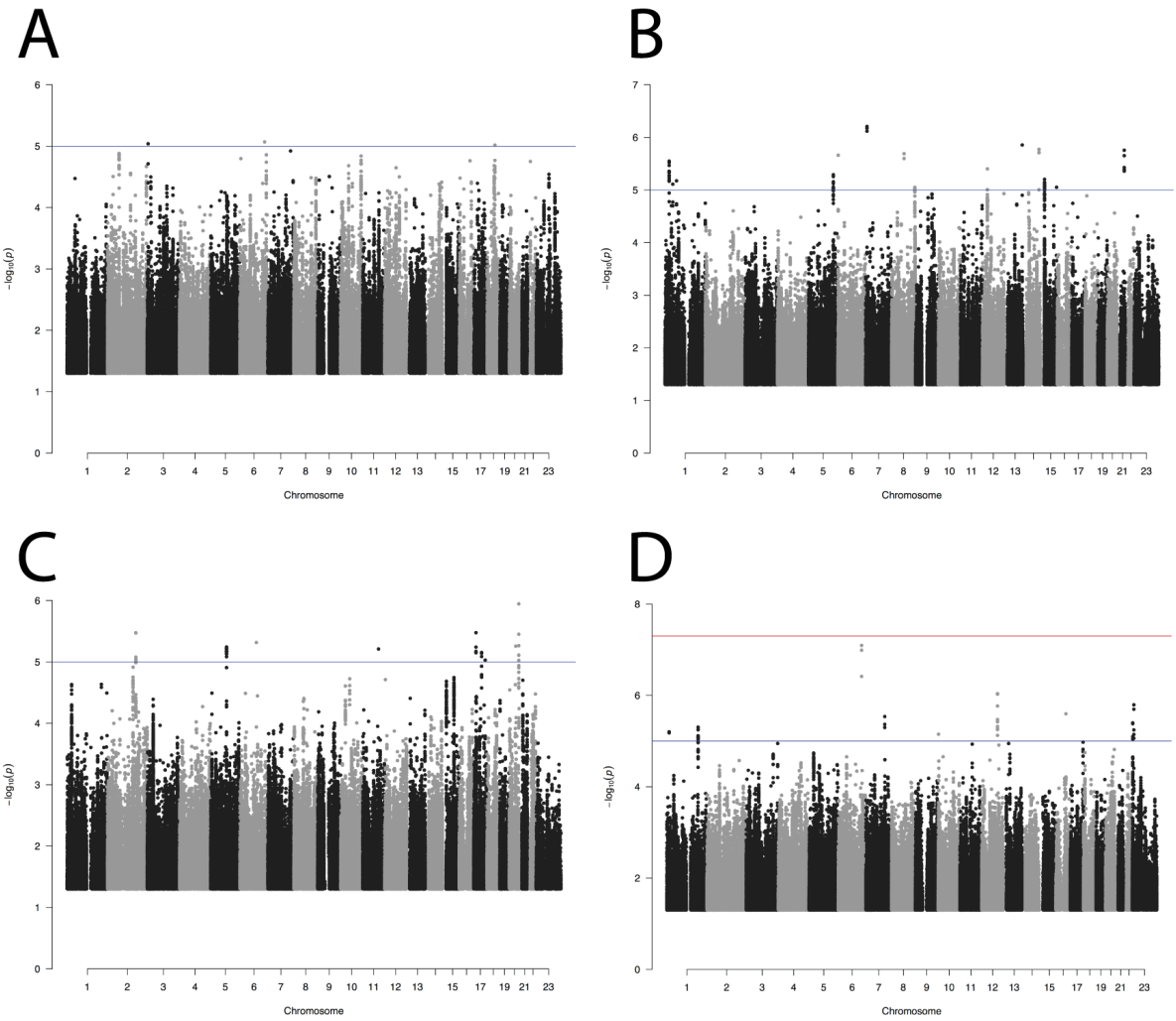


**Figure S5**: MacTel interaction GWAS results. A) Manhattan plot showing SNP interactions with GP serine, B) Manhattan plot showing SNP interactions with GP glycine, C) Manhattan plot showing SNPs interaction with SNP rs73171800 in locus 5q14.3, D) Manhattan plot showing SNP interactions with GP T2D.

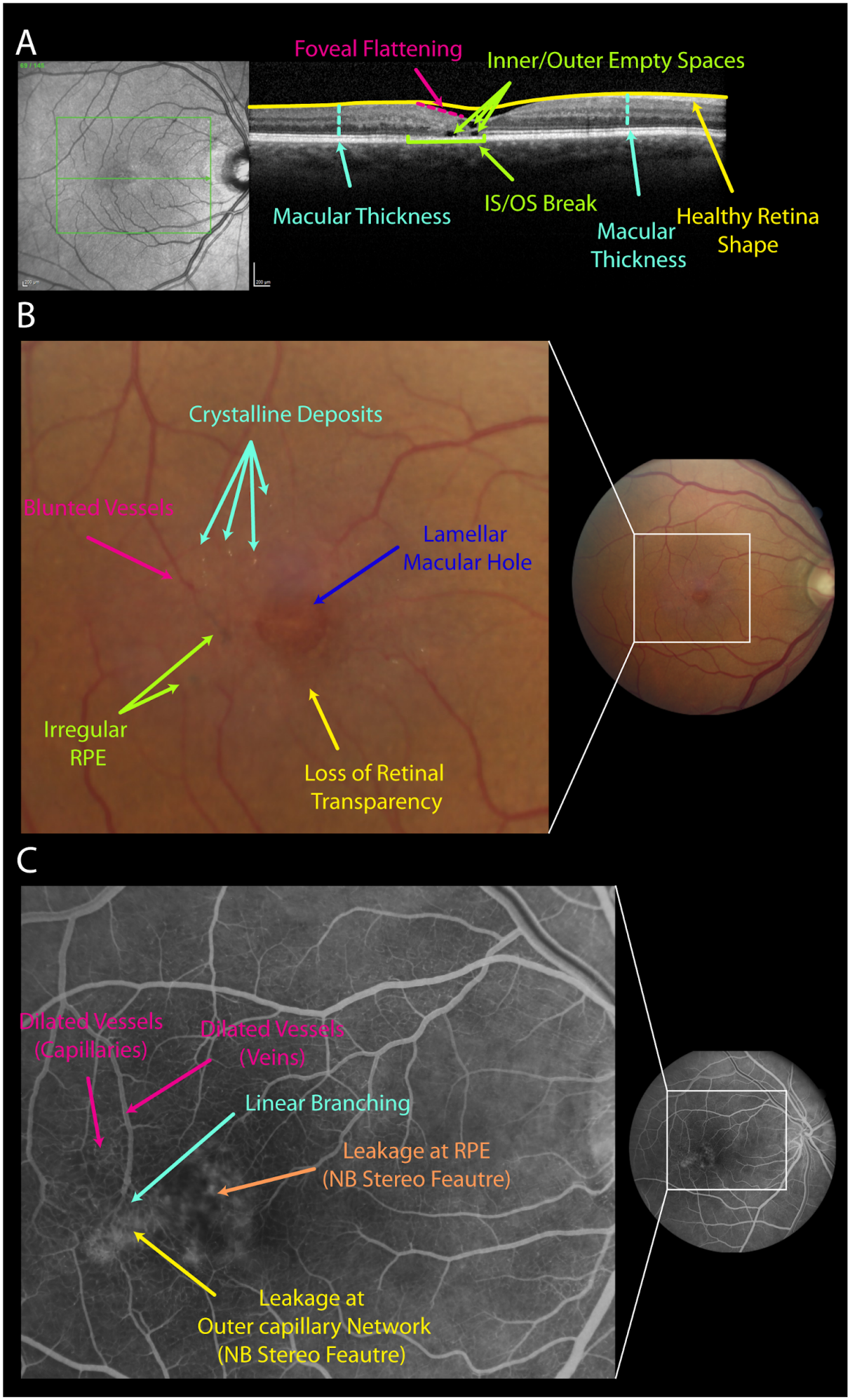
A
Foveal Flattening
Inner/Outer Empty Spaces
Macular Thickness
IS/OS Break
Macular Thickness
Healthy Retina Shape
B
Crystalline Deposits
Blunted Vessels
Lamellar Macular Hole
Irregular RPE
Loss of Retinal Transparency
C
Dilated Vessels (Capillaries)
Dilated Vessels (Veins)
Linear Branching
Leakage at RPE (NB Stereo Feautre)
Leakage at Outer capillary Network (NB Stereo Feautre)

**Figure S6:** Visual representation of the endophenotypes. A: Endophenotypes created from OCT scans. B: Endophenotypes created from fundus reflectance colour scans. C: Endophenotypes created from fundus fluorescein angiography. In this figure each endophenotype has a unique colour, the same colour in different images modality indicate different endophenotypes.

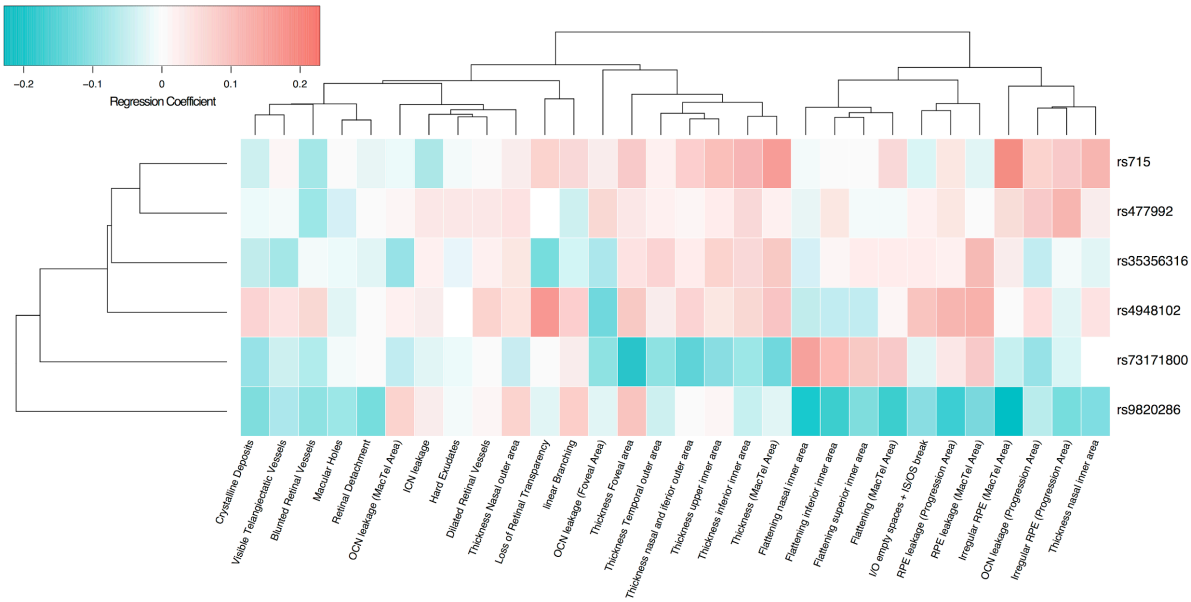


**Figure S7:** Loci clustering heatmap. This clustering heatmap visualises the regression coefficients of each SNP on the endophenotypes. Rows and columns of the heatmaps were ordered according to the hierarchical clustering to give a visual representation of the similarities. SNP rs73171800 (5q14.3) and SNP rs9820286 (3q21.3) have very different effects from the other four SNPs which show a more consistent, shared pattern.

# Supplementary Tables:

**Table S1:** SNPs and weights used to create GPMs, GPTs, Shin et al GPMs and MTAG serine (available as .xlsx file).

**Table S2:** List of all phenotypes and measurement methods used to create the endophenotypes (available as .xlsx file).

**Table S3:** List of all GPMs associations and conditional GPMs association results (available as .xlsx file).

**Table S4:** List of all Shin et al GPMs associations results (available as .xlsx file).

**Table S5:** Detailed FUMA output from MTAG analysis (available as .xlsx file).

**Table S6:** Endophenotypes analysis results (available as .xlsx file).

**Table S7:** Endophenotypes compositions and weights (available as .xlsx file).

**Table S8:** Members of the MacTel Project consortium (available at the end of this file).

# Supplementary Methods:

## GPM score calculation

We used the formula $GP(M/T)_i = \sum_{j \in i} \quad m_j * SNP_j$, where $GP(M/T)_i$ is the genetically predicted metabolite (*M*) or trait, *T*$i$. $SNP_j$ is the $jth$ SNP that was significantly associated with the metabolite or trait $i$. $m_j$ is the magnitude (weight) that the $SNP_j$ has on the metabolite or trait. The weight $m_j$ was obtained as $m_j = \beta_j$ where $\beta_j$ is the linear coefficient of the regression of $SNP_j$ on the metabolite or trait $i$. We used a total of 499 SNPs to predict the abundances of 142 metabolites in blood serum, 37 SNPs to construct a genetically predicted T2D risk, 5 for retinal venular calibre and 2 for the retinal arteriolar calibre. GPMs and GPTs were normalized to have a mean of zero and unit standard deviation.

# Imputation of phenotypic data

The phenotyping dataset contained multiple missing data points. Most missingness was related to imperfections in the ophthalmological images. By assuming missingness at random we imputed the missing data using predictive mean matching through chained equations, available in the package MICE [2].

# Generation of Endophenotypes with Factorial Analysis

The phenotypic data was summarised into endophenotypes. Endophenotypes have been defined as “measurable components unseen by the unaided eye along the pathway between disease and distal genotype”[3]. To identify and construct these underlying endophenotypes while ensuring that each only contained phenotypes strongly related to each other, we used an iterative factorial analysis algorithm. Given the very different nature of the phenotypes observed we performed two separate analyses for the creation of the endophenotypes one to capture macular thickness endophenotypes, and the other to capture macular abnormality phenotypes.

Starting with 43 phenotypic measurements for macular thickness and 76 for macular abnormality phenotypes we reduced these two data sets further, by only retaining correlated phenotypes within each dataset.
We discarded all those phenotypes/variables which:

- Had an absolute value of Spearman correlation with all other variables less than 0.3.
- Had an absolute value of Spearman correlation with the overall dataset score of less than 0.3.
- Would decrease the Cronbach's alpha of the dataset

This procedure retained 33 phenotypes for macular thickness and 52 phenotypes for macular abnormalities. Variables that were retained after this step underwent an iterative factorial analysis procedure:

1. Perform a *parallel analysis* on the dataset to discover the number of factors $F$ needed to summarise the phenotypic data
2. Run a *factorial analysis* with $F$ number of factors
3. Rotate the factors using the *oblimin* rotation to allow for correlation between endophenotypes and obtain a loading value for each phenotype in each factor.
4. Create a sequence of loading thresholds $T$ from 0.2 to 0.5 by 0.01
5. For each loading threshold $t \in T$ and for each factor $f \in F$, create a dataset that contains all the phenotype that have a loading greater than $t$. This results in F datasets.
6. Calculate the Cronbach's alpha in each dataset assessing the reliability of each factor.
7. Calculate the average of all factor’s alphas
8. Select the loading threshold $t*$ that maximize the average alpha.

9. Eliminate from the dataset all the variables that do not have any loading greater than $t*$.
10. Eliminate all variables which create factors by themselves.
11. Repeat 1-10 the entire process until no variables are removed.

This procedure was followed by an additional step, where we took the phenotypes that were discarded from the previous step and re-introduced into the endophenotype creation process, by themselves. Those phenotypes that were discarded a second time, were manually collapsed into meaningful new endophenotypes from previous clinical knowledge. These endophenotypes were obtained by simply summing the phenotypes values together.

Each factor created by this process was considered an endophenotype in further analysis. All endophenotypes resulted in continuous variables for which higher values represented negative impacts on patient's eye health. Specifically, higher values of macular thickness endophenotypes represented a risk of macular thinning, higher values for foveal slopes endophenotypes represented increase risk of foveal flattening, and higher values for macular abnormalities endophenotypes represented an increased risk of observing that particular endophenotype. Most of the analyses to obtain the endophenotypes were performed using the R package Psych[4].

Following the method used by [5], we also created foveal slope measurements from each parafoveal area using the macular thickness endophenotypes. The formula used is was $Slope_j = tan^{-1}((Thick_j - Thick_1)/500)$. Where $Slope_j$ indicates the slope from the fovea to the parafoveal area $j$and$Thick_j$is the endophenotype of macular thickness in area $j$. Since the foveal slope is defined as the slope from the fovea to the parafoveal areas the only areas used were area 2, area 3, area 4, and area 5 of the ETDRS grid.

The factorial analysis results in 9 endophenotypes describing macular thickness and 19 describing macular abnormalities. We discarded one macular thickness endophenotype and one macular abnormalities endophenotype since they were believed to describe only a residual correlation between phenotypes and have no real clinical relevance. Additionally, we obtained 4 endophenotypes describing macular slope leading to a total of 30 endophenotypes to be used in the analysis.

# Testing the identified disease key drivers and SNP loci against the endophenotypes

Endophenotypes were normalized to have zero average and unit standard deviation. Given the longitudinal nature of the data, we chose a linear mixed model approach to take into account the relationships within the subject and eye observation. Each model included all factors of interest as well as time defined as the number of days from the initial visit date, a quadratic function of visit year, gender, and age as covariates. Each model also contained a

885 random intercept and random time slope for each subject as well as a random intercept and
886 random time slope for each eye within each subject. We included all these random effects
887 since the log-likelihood of models that contained them and models which did not were
888 significantly different (results not shown. Models that compared fixed effects were estimated
889 using restricted maximum likelihood estimation. Given the large sample size, the p-values
890 were obtained by assuming the asymptotic normality property of the t-values for each
891 association. To take into account false discovery rate we used an adaptive Benjamini-
892 Hochberg procedure [6]. We adopted this procedure rather than strict Bonferroni correction
893 because of the very conservative nature of the linear mixed model and the small magnitude
894 of SNP effect sizes.
895
896
897

# 898 Supplementary Results:

899

## 900 Using MTAG to increase discovery power on GP serine

901 The much higher powered discovery GWAS for glycine and serine were used to predict glycine
902 and serine GPMs. The samples sizes for these two traits were different: (nGlycine = 79,293
903 and nSerine=30,68). For this reason, we tried to increase the discovery power of the serine
904 GWAS by using MTAG and combining serine GWAS results with the glycine GWAS results,
905 leveraging the genetic correlation between them (**Figure 1A**). Although MTAG estimated the
906 genetic correlation between the two traits to be high (0.413), the maximal FDR for serine was
907 also high (0.246). This was most likely caused by the difference in sample sizes of the two
908 studies. By using the results from this analysis, we constructed GP MTAG serine and tested
909 it for significance alongside GP glycine on MacTel. This resulted in a slight decrease of
910 significance for GP MTAG serine (p=6.24e-13) and a complete loss in significance for the
911 glycine original GPM (p=0.907).
912

## 913 MR using Shin et al 2014 metabolomics study:

914 We also tried to perform MR testing on all metabolites available from one of the first studies
915 on the genetic impact on metabolomics abundances by Shin et al 2014 [7,8] which contained
916 many more metabolites than those initially available to us. Of the 248 GPMs available we
917 found few additional metabolites to be significant (**Table S4**), None of them was as strongly
918 associated as GP glycine and GP serine and none retained significance after their inclusion
919 as covariates.

## 920 Composition of the endophenotypes

921 An illustrative image of the endophenotypes is presented in **Figure S6** while a detailed list of
922 phenotypes and respective loadings values used to estimate each of the endophenotypes is
923 available in **Supplementary Materials** and **Table S7**. Interestingly, among the 30 retained

endophenotypes, we noticed that some distinguished between abnormalities occurring in the initial MacTel region (area 5 in the ETDRS grid) and abnormalities expanding to the surrounding areas of the retina, which is usually denoted to indicate progression of the disease (areas 2, 3 and 4 on the ETDRS grid). For this reason, we defined these endophenotypes as "MacTel area" and "Progression" respectively.

## Supplementary Table 8:

| **The Emmes Corporation:**<br>***Coordinating Center***<br>401 N. Washington Street, Suite 700, Rockville, Maryland 20850<br>**Tel: 301.251.1161**<br><br>**MacTel@emmes.com** | | |
|---|---|---|
| Sarah Duwel, RN MA CCRA<br>*Principal Investigator / Project Director*<br>Tel: x10874 | Traci Clemons, PhD<br>*Principal Investigator / Statistician*<br>Tel: x10212 | Clay Styer<br>*Data Manager*<br>*Advantage eClinical*<br>Tel: x 17345 |
| Alexa Irazabal<br>*Administrative Coordinator – Genetic Shipping Supplies*<br>Tel: x10860 | Lena Bradley<br>*Project Manager – Lead CRA*<br>Tel: x10865 | |

| **Lowy Medical Research Institute**<br>***Executive and Fiscal Sponsor***<br>L31, 85 Castlereagh Street Sydney, New South Wales, AU | | |
|---|---|---|
| **Primary Contact:**<br>Jennifer Trombley RN MSN CCRC<br>*Director, Clinical Operations*<br>3366 N. Torrey Pines Ct., Suite 300<br>La Jolla, CA 92037<br>858.249.7109 office (US)<br>760.666.0452 mobile (US)<br>JTrombley@LMRI.net | Martin Friedlander MD PhD<br>*President – LMRI*<br>858.249.7100 office (US)<br>760.666.0452 mobile (US)<br>MFriedlander@LMRI.net | Anton Lever<br>*Group Manager, Finance*<br>AUS Tel: +612 9295 6015<br>AUS Mobile:<br>+614 0307 2143<br>alever@lfg.com.au |

| moorfields Reading Centre | Columbia University, Genetics Lab |
|---|---|
| *Moorfields Eye Hospital NHS*<br>*162 City Road*<br>*London EC1V 2PD*<br>MacTel@moorfields.nhs.uk | *Eye Institute Research Annex, Rm. 202*<br>*635 West 165th Street*<br>*New York, NY 10032*<br>*Tel: 212-305-8989* |
| Main contact:<br>**Konstantinos Balaskas**<br>**Consultant Ophthalmic Surgeon**<br>Konstantinos.Balaskas@moorfields.nhs.uk<br><br>**Administration:**<br><br>**Norma Jack**<br>**Tel: 020 7566 2815**<br>Norma.Jack@moorfields.nhs.uk | Main Contact:<br>**Carolyn Cai, Research Assistant**<br><br>Tel: 212-305-8501<br>Fax 212-305-7014<br>Cc3529@cumc.columbia.edu |

| Sites | | |
|---|---|---|
| Site Name | Principal investigator | Coordinator |
| Centre for Eye Research (002)<br>Australia Macula Research Unit<br>Level 1, 32 Gisborne St.<br>East Melbourne VIC 3002 | Robyn Guymer, PhD<br>Tel: 61 3 9929 8393<br>Fax: 61 3 9662 3859<br>Email:<br>rhg@unimelb.edu.au | Melinda Cain<br>Tel: 61 3 9929 8396<br>Email:<br>mcain@unimelb.edu.au<br><br>**EMILY CARUSO**<br>Tel: 61 3 9929 8113<br>Email:<br>emily.caruso@unimelb.edu.au |

| | | |
|---|---|---|
| Hôpital Lariboisière (004)<br>Service d'Ophtalmologie<br>2, rue<br>Ambroise<br>Paré,<br>Cedex 10<br>Paris<br>75475 | Alain Gaudric, MD<br>Tel: 33 1 4995 6480<br>Fax: 33 1 4995 6484<br>Email: alain.gaudric@aphp.fr | Abir Zureik<br>Tel: 33 1 49 95<br>64 86<br>Fax: 33 1 49<br>95 64 83<br>Email: abir.zureik@aphp.fr |
| Jules Stein Eye Institute, UCLA (005)<br>100 Stein Plaza, Room 2-565<br>Los Angeles CA,<br>90095 | Jean-Pierre Hubschman, MD<br>Tel: 310-206-5004<br>Fax: 310-825-3350<br>Email: hubschman@jsei.ucla.e | Rosaleen Ostrick<br>Tel: 310-794-5595<br>Fax: 310-794-5591<br>Email: ostrick@jsei.ucla.edu<br><br>Veronika Sadykov<br>Tel: 310-794-5596<br>Fax: 310-794-5591<br>Email:<br>Sadykov@jsei.ucla.edu<br>Mary Crowley<br>Tel: 310-267-5278<br>Email:<br>MECrowley@mednet.ucla.e<br>du |
| Lions Eye Institute (006)<br>2 Verdun Street<br>Nedlands WA 6009 | Ian Constable, MD<br>Tel: 61 8 9381 0882<br>Fax: 61 8 9381 0883<br>Email:<br>ian.constable@lei.org.au | Gareth Cooper<br>Email: GarethCooper@lei.org.au<br><br>Diana Bowman<br>Tel: +61 8 9381 0777<br>Fax: +61 8 9381 0700<br>Email: DianaBowman@lei.org.au |

| | | |
|---|---|---|
| Vitreous, Retina, MACULA Consultants of New York (007)<br>460 Park Avenue<br>5th Floor<br>New York, NY 10022 | Lawrence A. Yannuzzi, MD<br>Tel: 212-605-3777<br>Fax: 212-607-3795<br>Email: layannuzzi@gmail.com | MAria Scolara<br>Email: mscolaro@vrmny.com<br><br>Samira Shirwa<br>Tel: 212-452-6929<br>Email: sshirwa@vrmny.com<br>Sariah R. Persaud<br>Tel: 212-452-6929<br>Email: sariahpersaud@vrmny.com |
| Moorfields Eye Hospital (008)<br>Clinical Trials Unit<br>162 City Road<br>London EC1V 2PD | Cathy Egan, MD<br>Tel: 44 20 7566 2262<br>Fax: 44 20 7608 6925<br>Email: catherine.egan@moorfields.nhs.uk | Supeetha david<br>Tel: 0207 566 2835<br>Email: Supeetha.David@moorfields.nhs.uk<br><br>Tjebo Heeren<br>Email: Tjebo.Heeren@moorfields.nhs.uk |
| Retina Associates of Cleveland, Inc. (010)<br>3401 Enterprise Parkway, Suite 300<br>Beachwood, OH 44122 | Lawrence Singerman, MD<br>Tel: 216-831-5700<br>Fax: 216-360-2196<br>Email: lsingerman@retina-assoc.com | Diane Weiss, RN<br>Tel: 216-831-5704 Ext. 244<br>Fax: 216-360-2196<br>Email: dew@retina-assoc.com |

| | | |
|---|---|---|
| Save Sight Institute (011) | Mark Gillies, MD, PhD<br>GPO Box 4337 (use 2001 zip)<br>8 MacQuarie Street<br>Sydney NSW 2000<br>Tel: 61 4 1206 0313<br>Fax: 61 2 9382 7318<br>Email: mark.gillies@sydney.edu.au | Stella Xu<br>Tel +61 2 9382 7309<br>Fax +61 2 93827278<br>Email: stella.xu@sydney.edu.au<br>Sharon McKenzie<br>Tel +61 2 9382 7309<br>Fax +61 2 9382 7278<br>Email: sharon.mckenzie@sydney.edu.au<br><br>Maria Williams<br>Tel +61 2 9382 7286<br>Fax +61 2 9382 7278<br>Email : maria.williams@sydney.edu.au<br><br>Liza Shilpakar<br>Liza.shilpakar@sydney.edu.au |
| Scripps HEalth (012)<br>Scripps Clinical Research<br>10666 N. Torrey Pines Rd<br>La Jolla, CA 92037 | Martin Friedlander, MD, PhD<br>Tel: 858-784-9138<br>Fax: 858-784-9135<br>Email: friedlan@scripps.edu | Jennifer Trombley, RN<br>Tel: 858-554-6678<br>Fax: 858-554-5016<br>Mobile: 760-492-6600<br>Email: Trombley.jennifer@scrippshealth.org |
| St. Franziskus Hospital (013)<br>St. Franziskus Hospital<br>Hohenzollernring 74<br>Muenster D-48145 | Daniel Pauleikhoff, Prof. Dr<br>Tel: 49 251 933080<br>Email: dapauleikhoff@muenster.de | elke attenberger<br>Email: elke.attenberger@uveitis-zentrum.de<br>Tel: 0251-9352758<br>Martin Ziegler<br>Email: mpz@alex-ziegler.de |

| | | |
|---|---|---|
| The Goldschleger Eye Institute (014)<br>The Chaim Sheba Medical Center<br>Tel Hashomer 52621 | Joseph Moisseiev, MD<br>Tel: 972 3 534 3462<br>Email:<br>Joseph.moisseiev@sheba.health.gov.il | Rinat Rashty<br>Tel: 972-3-530 2877<br>Email:<br>Rinat.rashty@sheba.health.gov.il |
| The New York Eye and Ear Infirmary (015)<br>Department of Ophthalmology<br>310 East 14th Street<br>Suite 319 South Building<br>New York NY, 10003 | Richard Rosen, MD<br>Tel: 212-979-4284<br>Fax: 212-979-4512<br>Email: rrosen@nyee.edu | **MELIZA UNSON**<br>Tel: 212-979-4672<br>Email: munson@nyee.edu |
| University of BONN (017)<br>Dept. of Ophthalmology<br>Ernst-Abbe-Str. 2<br>Bonn, 53127 | Frank Holz, MD<br>Tel: 49 228 287 5647<br>Fax: 49 228 287 5603<br>Email:<br>Frank.Holz@ukbonn.de | Simone Müller,<br>Assistenzärztin<br>Email:<br>Simone.Mueller@ukbonn.de<br><br>**Kerstin Bartsch**<br><br>Email:<br>Kerstin.Bartsch@ukbonn.de |
| University of Michigan,<br>Kellogg Eye Center (019)<br>1000 Wall Street<br>Ann Arbor MI, 48105 | Grant Comer, MD<br>Room 714<br>Tel: 734-763-5906<br>Fax: 734-936-2340<br>Email: gcomer@umich.edu | Pam Campbell, COT, CCRP<br>Room 1415<br>Tel: 734-936-0138<br>Email:<br>pamtitus@med.umich.edu |
| Scheie Eye Institute (022)<br>51 North 39th Street<br>Philadelphia PA, 19104 | Alexander Brucker, MD<br>Tel: 215-662-8675<br>Fax: 215-662-8025<br>Email:<br>ajbrucke@mail.med.upenn.edu | Sheri Drossner<br>Tel: 215-662-8177<br>Fax: 215-662-8025<br>Email:<br>Sheri.Grand@uphs.upenn.edu |
| University of Bern (024)<br>Universitätsklinik für Augenheilkunde<br>Inselspital<br>Bern<br>, CH<br>3010 | Sebastian Wolf, MD, PhD<br>Tel: 41 (0)31 632 8503<br>Fax: 41 (0)31 632 4382<br>Email:<br>Sebastian.wolf@insel.ch | Corinne Stockli<br>Tel: 41 (0)31 632 1197<br>Fax: 41 (0)31 632 0114<br>Email:<br>Corinne.Stoeckli@insel.ch |

| | | |
|---|---|---|
| University of Utah Health Care (025)<br>Moran Eye Center<br>University of Utah Health Care<br>65 Mario Capecchi Drive<br>Salt Lake City, UT 84132 | Paul Bernstein, MD, PhD<br>Tel: 801-581-6078<br>Fax: 801-581-3357<br>Mobile: 801-560-3093<br>Email: paul.bernstein@hsc.utah.edu | Barbara Hart<br>Email: Barbara.hart@hsc.utah.edu<br><br>Kara Halsey<br>Tel: 801-213-2034<br>Email: Kara.halsey@utah.edu<br><br>Kimberly Wegner<br>Tel: 801-584-6265<br>Email: Kimberley.wegner@hsc.utah.edu<br><br>Sam Taylor<br>Email: samclarktaylor@gmail.com<br><br>**ELIZABETH NUTTALL – Regulatory Documents**<br><br>Email: Elizabeth.nuttall@hsc.utah.edu |
| Bascom Palmer (Miami) (026) | Philip Rosenfeld, MD, PhD<br>900 NW 17th Street<br>Miami FL, 33136<br>Tel: 305-326-6148<br>Fax: 305-326-6538<br>Email: prosenfeld@med.miami.edu | Cristina Lage-Rodriguez, MS, CCRC<br>1638 NW 10th Avenue, Suite 505B<br>Miami, FL 33136<br>Tel: 305-326-6117<br>Fax: 305-547-3662<br>Email: clage@med.miami.edu |
| Massachusetts Eye and Ear (027)<br>Retina Service<br>243 Charles Street<br>Boston, MA 02114 | Joan Miller, MD<br>Tel: 617-573-3915<br>Fax: 617-573-3364<br>Email: joan_miller@meei.harvard.edu | Patricia Houlihan<br>Tel: 617-573-3646<br>Fax: 617-573-3514<br>Email: patricia_houlihan@meei.harvard.edu<br><br>Alex Leite<br>Email: Alex_Leite@meei.harvard.edu |
| Emory University (028)<br>Emory Eye Center<br>1365B Clifton RD NE<br>Atlanta, GA 30322 | Jiong Yan, MD<br>Tel: 617-573-3915<br>Email: jyan2@emory.edu | Jayne Brown<br>Tel: 404-778-4430<br>Email: jmbrown@emory.edu |

| | | |
|---|---|---|
| UNiversity of California – San francisco (029)<br>UCSF Department of Ophthalmology<br>10 Koret Way Box 0730, Room K209<br>San Francisco, CA 94143 | JaCque Duncan, MD<br>Tel: 415-514-4241<br>Email: jacque.duncan@ucsf.edu | Arshia MiaN<br>Email: Arshia.Mian@ucsf.edu<br><br>MARY LEW<br>Email: Mary.Lew@ucsf.edu |
| University of Rochester (030)<br>Flaum Eye Institute<br>601 Elmwood Avenue Box 659<br>Rochester, NY 14642 | Mina Chung, MD<br>Tel: 585-275-4141<br>Email: mina_chung@urmc.rochester.edu | Katherine Nedrow<br>Tel: 585-275-9485<br>Email:katherine_nedrow@urmc.rochester.edu |
| Medical College of Wisconsin (031)<br>The Eye Institute<br>925 N. 87th Street, Room 807<br>Milwaukee, WI 53226 | David Weinberg, MD<br>Tel: 414-955-2026<br>Email: dweinber@mcw.edu | Ellie Dorsey<br>Tel: 414-955-7854<br>Email: edorsey@mcw.edu<br><br>Shay Bourgeois<br>Tel: 414-955-2001<br>Email: sbourgeois@mcw.edu<br><br>B**rittany Rego**<br>Tel: 14-955-2031<br>Email: brego@mcw.edu |
| Radboud (033)<br>Radboud University Medical Center<br>Departments of Ophthalmology & Human Genetics<br>P.O. Box 9101, 6500 HB Nijmegen (409) | CB Hoyng, MD<br>Email: trialcentrum.ohk@radboudumc.nl<br>Tel: +31 (0)24 36 15255 | Asha Kalisingh<br>Email: asha.kalisingh@radboudumc.nl<br>Tel: + 0243613212<br><br>chantal jumelet vanast<br>Email: Chantal.Jumelet-vanAst@radboudumc.nl<br><br>Clasien Oomen – regulatory<br>Email: clasien.oomenvanast@radboudumc.nl<br>Tel: + 31-24-36 15255 |
| Oxford eye hospital (034)<br>John Radcliffe Hospital West Wing | **Peter Charbel Issa MD, DPhil, FEBO**<br><br>T: 01865 227678 | Alexina Fantano<br>T: 01865 231053<br>F: 01865 231160<br>Email: alexina.fantato@ouh.nhs.uk |

| | | |
|---|---|---|
| Headley Way,<br>Headington, Oxford,<br>OX3 9DU | Email:<br>peter.charbelissa@ndcn.ox.ac.uk | |
| Eye Center, Medical Center, Faculty of Medicine, University of Freiburg (035)<br>German: Klinik für Augenheilkunde, Universitätsklinikum Freiburg<br><br>UNIVERSITÄTSKLINIKUM FREIBURG<br>Klinik für Augenheilkunde<br>Studienteam der Sektion Retinologie<br>Dagmar Rommel<br>Studienassistentin / Studienkoordination<br>Killianstraße 5 · 79106 Freiburg /Germany<br>Telefon: 0761 270-40231<br>Telefax: 0761 270-86210 | Felicitas Bucher, MD<br>Email: bucherf@scripps.edu | Dagmar Rommel<br>Email: dagmar.rommel@uniklinik-freiburg.de |
| Retina Research CEnter (036)<br>3705 Medical Parkway<br>Suite 420<br>Austin, Texas 78705 | Chirag Jhaveri, Md<br>Email: cjhaveri@e-retina.net<br>Tel: 512-279-1251 | ivana Gunderson<br>Email: igunderson@e-retina.net<br>Tel: 512-279-1251<br><br>Daniela Rodridguez<br>Email: drodriguez@e-retina.net |

| | | |
|---|---|---|
| Retina Consultants of Southern Colorado (037)<br>2770 N. Union Blvd.<br>Suite 140<br>Colorado Springs, CO 80909 | Ryan Rich, MD<br>Email: researchmdrich@coloradoretina.com<br>Tel: 719-473-9595 | Jordan Townsend<br>719-473-9595 Ext. 123<br>Email: jtownsend@coloradoretina.com<br><br>Dragana Kuga<br>Email: dkuga@coloradoretina.com<br>Victoria Lee<br>Email vlee@coloradoretina.com<br><br>Kari Winger<br>Email kwinger@coloradoretina.com |
| Cincinnati Eye Institute – CEI Physicians PSC, Inc (038)<br>1945 CEI Drive<br>Cincinnati, OH 45242 | Daniel Miller, MD<br>Email: dmiller@cincinnatieye.com<br>Tel: 513-569-3669 | Megan Kingdon, RN, BSM, CCRC<br>Email: mkingdon@cincinnatieye.com<br>Tel: 513-569-3669<br><br>Kelsi Dwyer<br>Email: kdwyer@cincinnatieye.com |
| University of Washington Eye Institute (039)<br><br>908 Jefferson St., 7th Floor, Seattle, WA 98104<br>Mailing Address: Box 359607, 325 Ninth Avenue, Seattle, WA 98104 | Cecilia Lee, MD<br>Email: jung.cecilia@gmail.com | Ian Luttrell<br>Email: luttri@uw.edu<br><br>Francy Moses<br>Email: mosesf@uw.edumary |
| Byers Eye Institute - Stanford University (040)<br>2370 Watson Court<br>Palto Alto, California 94303 | Diana Do, MD<br>Email: dianado@stanford.edu<br>Tel: 650-723-6995 | Lisa Greer<br>Email: lgreer7@stanford.edu<br>Tel: 650-725-9184 |

| | | |
|---|---|---|
| | | |
| MAyo Clinic (041)<br>200 First St SW<br>Rochester, MN 55905 | Sophie Bakri, MD<br>Email:<br>bakri.sophie@mayo.edu | Heidi Rubin<br>Email:<br>Rubin.heidi@mayo.edu |
| Retina Center of New Jersey, LLC (042)<br>1255 Broad Street, Suite 104<br>Bloomfield, NJ 07003 | Patrick Higgins, MD<br>Email:<br>Drhiggins@Retinacenternj.Com<br>Tel: 973-707-5632 | Diane Deininger<br>Email:<br>ddeininger@retinacenternj.com<br>Tel: 973-707-5632<br>Fax :973-337-5865<br>Susan Anderson<br>Email:<br>sanderson@retinacenternj.com<br>Tel: 973-707-5632<br><br>Valerie Benavides<br>Email:<br>vbenavides@retinacenternj.com<br>Tel: 973-707-5632<br>KAthleen Rodriguez<br>Email:krodriguez@retinacenternj.com<br>Tel: 973-707-5632 |
| Retina Associates New Orleans (043)<br>4315 Houma Boulevard Suite 201<br>Metairie, LA 70006 | Stanislav A. Zhuk, MD, FACS<br>Email:stanislav.zhuk@retinaassociates.org<br>Tel: 504-456-9061<br>Fax: 504-895-8094 | MElinda Mitchell<br>Email:<br>Melinda.mitchell@retinaassociates.org |

| | | |
|---|---|---|
| Royal Oak (044)<br><br>Associated Retinal Consultants, P.C.<br>Neuroscience Center Building<br>3555 West Thirteen Mile Road Ste. LL-20<br>Royal Oak, MI 48073 | Sandeep Randhawa | Kendra Mellert<br>E-mail: kmellert@arcpc.net<br>Tel: 248-288-9132 ext. 1313<br>Fax: 248-288-2265 |
| Grand Rapids (144)<br><br>Associated Retinal Consultants, P.C.<br>1179 East Paris, S.E.; suite: 250<br>Grand Rapids, MI 49546 | Paul V. Raphaelian, M.D. | Deb Markus<br>Email: dmarkus@arcpc.net |
| Traverse City (244)<br><br>Associated Retinal Consultants, P.C.<br>860 E. Front St.<br>Traverse City, Mi 49686 | Scott Sneed | Serena Neal<br>Email: sneal@arcpc.net |
| Sierra Eye Associates (045)<br>950 Ryland Street,<br>Reno, NV, 89502 | Arshad Khanani, MD<br>Email: arshad.khanani@gmail.com<br>Tel: 775-329-0286 | Deanna Dorman<br>Email:ddorman@sierraeyeassociates.com<br>Tel: 775-329-0286 x 141<br><br>**Heather Southwick**<br>Email: hpopovich@sierraeyeassociates.com |

| | | |
|---|---|---|
| Retina Northwest – PORTLAND (046)<br>Portland<br>5440 SW Westgate Drive Suite 217<br>Portland, OR 97221 | Michael Lee, MD<br>Email: MLee@retinanorthwest.com<br>Tel: 503-274-2121 | Brian Puckett<br>Email: bpuckett@retinanorthwest.com<br>Tel: 503-274-2121<br>Fax: 503-229-8472 |
| Eramus - Netherlands (047)<br>Department of Ophthalmology<br>Erasmus Medical Center Rotterdam<br>BA-130 postvak 'Trials'<br>3000 CA Rotterdam<br>The Netherlands | J. Vingerling, MD<br>Email: j.vingerling@erasmusmc.nl | MARjo-Lan jansen<br>Email: m.jansen-vandrecht@erasmusmc.nl |
| New England Retina Consultants, PC (048)<br>3640 Main Street, Suite 201<br>Springfield, MA. 01107 | David LaLLY, MD<br>Email: david.lally@gmail.com | Leah Persky<br>Email: persky.leah@gmail.com<br>Tel: 413-788-6044<br>Fax: 413-746-9715 |
| CUMBERLAND VALLEY RETINA CONSULTANTS (049)<br>1150 Opal Court<br>Hagerstown, MD 21740 | DAVID WARROW, MD<br>Email: Davidw@retinacare.net | Paula SMith<br>Email: paulas@retinacare.net<br>Tel: 301-665-1712<br>Fax: 301-655-1714<br><br>Katie Alvord<br>Email: katiea@retinacare.net<br>Tel: 301-665-1712 x 1024 |

| | | |
|---|---|---|
| Northwestern University (050)<br>259 E. Erie, Suite 15-20,<br>Chicago, IL 60611 | Amani Fawzi, MD<br>Email: amani.fawzi@northwestern.edu | Regulatory:<br>Michell Kim<br>Email: michell.kim@northwestern.edu<br>Tel:312-503-2229<br><br>Nicole Seddon<br>Email: nreinhol@nm.org<br>Tel: 312.695-0252<br><br>Priya Thakkar<br>Email: Priya.Thakkar@nm.org<br>Tel: 312.695.2573 |
| ZNA Middelheim Hospital (051)<br>Lindendreef 1<br>2020 Anterwerp, Belguim | Joke Ruys, MD<br>Email: joke.ruys@zna.be<br>Tel : +0032 3 280 3614 | LiEsBeth VanPeene<br>Email: liesbeth.vanpeene@zna.be<br>Tel. +0032 3 280 3614 |
| Bay Area Retina Associates (052)<br>122 La Casa Via Suite 223<br>Walnut Creek, CA 94598 | Roger Goldberg, MD<br>Email:rgoldberg@bayareaetina.com | Farhan AhmeD<br>Email:fahmed@bayareaetina.com |
| Southeastern Retina Associates, P.C. (053)<br>1124 E. Weisgarber Rd. \| Suite 207<br>Knoxville, TN 37909 | Joseph M. Googe Jr, MD<br>Email: ctgooge@seretina.com<br>Tel: 865-588-0811 | Kristina Oliver<br>Email: koliver@seretina.com |
| Mayo Clinic, Scottsdale Arizona (054)<br>13400 East Shea Boulevard<br>Scottsdale, AZ 85259 | Odette Houghton, MD<br>Email: Houghton.Odette@mayo.edu | Michaele Menghini<br>Email: Menghini.Michaele@mayo.edu |

| | | |
|---|---|---|
| Elman Retina Group, P.A. (055)<br>9114 Philadelphia Rd.<br>Suite 310<br>Baltimore, MD 21237 | Michael J. Elman, M.D.<br>Email:<br>elman@elmanretina.com<br>Phone: 410- 686-3000<br>Fax: 410- 686-3690<br>Cell: 410-812-6440 | JoAnn Starr<br>Email:<br>Starr@elmanretina.com<br>Phone: **410-686-3000**<br>FAX**: 410-686-3690** |
| Retina Consultants of Houston (056)<br>6560 Fannin Street<br>Suite 750<br>Houston, TX 77030 | Charles Wykoff, MD, PhD<br>Email :<br>ccwmd@houstonretina.com<br>Phone: 713-524-3434 | Kirsten Poldervart<br>Email:<br>kirsten.poldervart@houstonretina.com<br>Phone: 713-524-3434<br><br>Jose Munoz<br>Email:<br>jose.munoz@houstonretina.com<br>Phone: 713-524-3434<br>Cassandra 'Cassie' Cone<br>Email:<br>Cassandra.cone@houstonretina.com<br>Phone: 713-524-3434<br><br>MArie Chin (Regulatory)<br>Email:<br>marie.chin@houstonretina.com<br>Phone: 713-524-3434 |
| Charles Retina (057)<br>1432 Kimbrough Road<br>Germantown, TN<br>38138 | Steve Charles, MD<br>Email: scharles@att.net | Melanie Woods<br>Email:<br>mwoods@charlesretina.com |
| Tulsa Retina Consulants (059)<br>2424 E 21st Street,<br>Suite 200<br>Tulsa, OK 74114<br>918-794-6089 | Lars Freisberg, MD<br>Email<br>Larsfreisberg@mac.com | Scott Hewitt<br>Email:<br>shewitt@retinatulsa.com<br>Phone: 918 -734-6344<br><br>Debbie Hardison<br>Email:<br>dhardison@retinatulsa.com |

| | | |
|---|---|---|
| Palmetto Retina Center, LLC (061)<br>124 Sunset Court<br>West Columbia, SC 29169 | JOHN A. Wells, III, MD<br>Email: jackwells@palmettoretina.com | Peggy Miller<br>Email: pmcdougal@palmettoretina.com<br>Phone: 803-404-5038<br>Fax: 803-744-0145<br><br>Mallie Taylor<br>Email: mtaylor@palmettoretina.com |
| Texas Retina Associates (062)<br>9600 N. Central Expressway, Suite 100<br>Dallas, TX 75231 | Gary Fish, MD<br>Email: gefgef@ix.netcom.com | Karen Duignan<br>Email : kduignan@texasretina.com<br>Phone: 214-692-6885 x1<br>Fax: 214-265-0935<br><br>Tiffanie Keaton<br>Email: tkeaton@texasretina.com |
| Ophthalmic Consultants of Long Island (063)<br>360 Merrick Rd<br>3rd Floor<br>Lynbrook, NY 11563 | Glenn Stoller, MD<br>Email : glstoller@gmail.com<br>Phone: 516-593-4026 | Brennon Taylor<br>Email: btaylor@ocli.net<br>Phone: 516-593-4026<br><br>Susan Jones<br>Email: sjones@ocli.net<br>Phone: 516-593-4026<br><br>Carla Del Castillo<br>Email : cdelcastillo@ocli.net<br>Phone: 516-593-4026 |

| | | |
|---|---|---|
| Center for Retina and Macular Disease - Central Florida (065)<br>**250 Avenue K, SW**<br>**Suite 200**<br>**Winter Haven, FL 33880** | Richard Hamilton<br>Email: rich@crmd.net | Research Supervisor<br>Toni Collins<br>Email: tocol@crmd.net<br>Phone: 863-297-5400 Ext. 2046<br><br>Tammy<br>Email: tamc@crmd.net |
| **Retina-Vitreous Associates Medical Group (066)**<br>**9001 Wilshire Boulevard, Suite 301**<br>**Beverly Hills, CA 90211** | David Boyer M.D.<br>Email: vitdoc@aol.com | Janet Kurokouchi<br>Email: JKurokouchi@laretina.com<br>Phone: (310) 289-2478 x 3 (main study line) |
| **Global Research Foundation (067)**<br>**7447 N Figueroa Street**<br>**Los Angeles, CA 90041** | **Khaled Tawansy**<br>Email: ktawansy@globalresearchgroup.net | Research Supervisor<br>Monica Torres<br>Email: mtorres@globalresearchgroup.net<br>Phone: 323-257-3300 ext 120 |

# References

1. Mathew R, Sivaprasad S, Florea D, et al. Agreement between time-domain and spectral-domain optical coherence tomography in the assessment of macular thickness in patients with idiopathic macular telangiectasia type 2. *Ophthalmologica*. 2013;230(3):144-150. doi:10.1159/000353455

2. Buuren S van, Groothuis-Oudshoorn K. mice: Multivariate Imputation by Chained Equations in R. 2011. http://doc.utwente.nl/78938/. Accessed March 10, 2017.

3. Gottesman II, Gould TD. The endophenotype concept in psychiatry: etymology and strategic intentions. *Am J Psychiatry*. 2003;160(4):636-645. doi:10.1176/appi.ajp.160.4.636

4. Revelle W. psych: Procedures for personality and psychological research. *Northwestern University, Evanston R package version*. 2014;1(1).

5. Jaisankar D, Raman R, Gondhale H, Chhablani J, Agarwal M. VISUAL FUNCTION CORRELATES OF FOVEAL SLOPE CHANGES ON OPTICAL COHERENCE TOMOGRAPHY IN MACULAR TELANGIECTASIA TYPE 2. *Retina*. December 2016. doi:10.1097/IAE.0000000000001416

6. Benjamini Y, Krieger AM, Yekutieli D. Adaptive linear step-up procedures that control the false discovery rate. *Biometrika*. 2006;93(3):491-507. doi:10.1093/biomet/93.3.491

7. metabolomics gwas server. http://metabolomics.helmholtz-muenchen.de/gwas/. Accessed December 4, 2018.

8. Shin S-Y, Fauman EB, Petersen A-K, et al. An atlas of genetic influences on human blood metabolites. *Nat Genet*. 2014;46(6):543-550. doi:10.1038/ng.2982